

# A Critical Evaluation of the Physical Nature of the Little Red Dots

KOHEI INAYOSHI <sup>1</sup> AND LUIS C. HO <sup>1,2</sup>

<sup>1</sup>*Kavli Institute for Astronomy and Astrophysics, Peking University, Beijing 100871, China*

<sup>2</sup>*Department of Astronomy, School of Physics, Peking University, Beijing 100871, China*

## ABSTRACT

Little Red Dots (LRDs) are a newly identified class of active galactic nuclei (AGNs) uncovered by JWST deep surveys. Their enigmatic properties challenge the canonical AGN paradigm and have stimulated numerous ideas on the early formation and growth mechanisms of massive black holes (BHs). In this review, we summarize how early BHs can shape the characteristic features of LRDs, how their nuclear environments differ from those of normal AGNs, and how future observations can distinguish between competing scenarios (AGN or stellar origins). Our main conclusions are as follows:

- LRDs show broad-line emission consistent with mass accretion onto BHs with  $M_{\text{BH}} \simeq 10^6 - 10^7 M_{\odot}$ , suggesting that AGN activity is a plausible origin of their dominant red optical emission.
- Stellar components can reproduce the continuum energetics through dusty star formation. However, the required stellar mass would be too large to remain consistent with other key LRD properties. Therefore, a purely stellar origin is unlikely to be the dominant power source, although star formation may still contribute to the UV emission.
- The coexistence of broad-line emission with Balmer absorption and break features on LRD spectra, neither of which can be explained by evolved stellar populations, suggests that nuclear BHs are enshrouded by dense gas with a high covering fraction.
- Gas-enshrouded AGNs can produce red optical spectra without requiring dust reddening through a combination of gas attenuation and thermal self-emission with an effective temperature of  $T_{\text{eff}} \simeq 5000$  K, which also accounts for the flat infrared continuum. This scenario therefore offers a compelling explanation, although alternative interpretations are discussed in this review.
- From the spectral features and redshift evolution, LRDs are likely a transient phase in early BH growth, possibly the first accretion episodes of newborn BHs.
- Testing models for LRD spectra and origins through exploring time variability, sources of ionizing radiation, post-LRD objects, and low-redshift LRD analogs is particularly promising.

*Keywords:* High-redshift galaxies (734) — Quasars (1319) — Supermassive black holes (1663)

## 1. INTRODUCTION

The James Webb Space Telescope (JWST) has opened an unprecedented window into high-redshift extragalactic astronomy. Thanks to its sensitivity and spatial/spectral resolution in the infrared (IR) bands, redshifted light from active galactic nuclei (AGNs) powered by accreting massive black holes (BHs) can be observed in detail, offering new insights into the nature and evolution of early BHs and their host galaxies. One of the most remarkable discoveries by JWST is a new population of AGNs known as little red dots (LRDs), compact sources with red optical continua and broad-line emission signatures. The first spectroscopically confirmed LRD, CEERS 746 at  $z = 5.624$ , was reported by Kocevski et al. (2023). Following this discovery, a slitless spectroscopic survey with JWST/NIRCam identified approximately 20 similar red sources exhibiting broad H $\alpha$  emission, earning them the nickname “Little Red Dots” (Matthee et al. 2024). Independent studies have reported additional LRDs from multiple JWST programs, including

CEERS (Harikane et al. 2023), JADES (Maiolino et al. 2024), UNCOVER (Greene et al. 2024), and ASPIRE (Lin et al. 2024) and confirmed that LRDs are a common and robust phenomenon in the early universe.

The discovery of LRDs has sparked considerable interest in both observational and theoretical communities, as LRDs may represent a previously unrecognized, early phase of BH accretion activity and thus potentially reshape our understanding of BHs and galaxy assembly. Importantly, LRDs appear to deviate from the standard AGN paradigm in several aspects, including their V-shaped UV-optical spectral energy distributions (SEDs) with a turnover wavelength around rest-frame  $\simeq 4000$  Å, their broad-line emission properties, and the weakness in canonical AGN signatures such as hot dust and X-ray corona emission. Moreover, LRDs host massive BHs likely heavier than the typical seed masses predicted by theory and simultaneously have substantially undermassive host galaxies. These features raise fundamental questions about their physical origin and role.

In the past three years since the initial discovery, a rapidly increasing number ( $\sim 500$ ) of LRDs has been identified. These findings have revealed several robust features, but also often delivered new and unexpected puzzles. Given the fast pace of developments and the daily appearance of new LRD-related papers, key results and interpretations can sometimes be overlooked, occasionally leading to some misconceptions. This review aims to summarize current observational and theoretical understanding of LRDs, clarifying what aspects are well established and what remain uncertain. We employ order-of-magnitude arguments to elucidate the governing physical processes, and outline major open questions that define the next frontier of this emerging field.

## 2. KEY CHARACTERISTICS

LRDs have drawn considerable attention due to a set of unique features that distinguish them from the population of previously known normal AGNs. In this section, we summarize their defining observational characteristics based on current data.

### 2.1. High-redshifts objects

We begin with the reminder that LRDs are confirmed to reside at high redshifts. Spectroscopic observations with JWST/NIRCam and NIRSpec unveil their redshift range as  $4 \lesssim z \lesssim 9$  (Matthee et al. 2024; Kokorev et al. 2024a; Kocevski et al. 2025), corresponding to cosmic times of  $t \simeq 0.5\text{--}1.5$  Gyr and luminosity distances of  $D_L \simeq 30\text{--}100$  Gpc. Their observed fluxes, combined with these distances, imply luminosities in the rest-frame UV and optical bands on the order of

$$\nu L_\nu^i = 4\pi D_L^2 (\nu F_\nu^i)_{\text{obs}} \simeq \begin{cases} 4.0 \times 10^9 L_\odot & \text{for } i = \text{UV}, \\ 1.2 \times 10^{10} L_\odot & \text{for } i = \text{optical}, \end{cases} \quad (1)$$

obtained from the panchromatic SED of the typical LRD (Akins et al. 2025a; Delvecchio et al. 2025), as shown in Figure 1. The typical uncertainty of the stacked flux is 8% in the UV band and 6% in the optical band. This estimate neglects any dust extinction and shows the observed values without correction. Applying dust extinction of  $A_\lambda$  at a wavelength of  $\lambda$  along with an attenuation law increases the inferred intrinsic luminosity by a factor of  $10^{0.4A_\lambda}$  as

$$\nu L_\nu^i \simeq \begin{cases} 6.3 \times 10^{10+0.4(A_{\text{UV}}-3)} L_\odot & \text{for } i = \text{UV}, \\ 1.9 \times 10^{11+0.4(A_V-3)} L_\odot & \text{for } i = \text{optical}, \end{cases} \quad (2)$$

where the extinction levels of  $A_V$  and  $A_{\text{UV}}$  are defined at rest-frame 5100 Å and 1500 Å, respectively. Therefore, the optical-to-UV luminosity ratio is expressed as

$$\frac{L_{\text{opt}}}{L_{\text{UV}}} \simeq 3.0 \times 10^{0.4(A_V - A_{\text{UV}})}, \quad (3)$$

where  $L_i = \nu L_\nu^i$  ( $i = \text{UV}$  and optical).

### 2.2. V-shaped SEDs

A distinct feature of LRDs is their V-shaped UV-to-optical SEDs. This shape is observed in the prototype LRD (CEERS 746, Kocevski et al. 2023) and has become a primary selection criterion using JWST broad- and medium-band

photometric colors (e.g., [Greene et al. 2024](#); [Kocevski et al. 2025](#); [Hainline et al. 2025](#)). Quantitatively, the SEDs can be described by a broken power law in the form  $F_\lambda \propto \lambda^\beta$ , with typical slopes of  $\beta_{\text{UV}} \simeq -2$  (UV part) and  $\beta_{\text{opt}} \simeq 0$  (optical part).

This spectral characteristic motivated interpretations assuming two components in early studies on LRDs:

- A blue UV slope from unobscured sources (young stellar populations or unobscured AGNs),
- A red optical slope from dust reddened, obscured sources (dusty galaxy or obscured AGNs).

Alternatively, a single AGN plays two effective roles:

- A red optical from dust reddened, obscured AGNs and a blue UV excess from scattered light (dust and electrons) leaking through a patchy, partially covering medium.

However, such two-component models generally face a fine-tuning problem. Despite significant variation in redshift, luminosity, and selection method, LRDs consistently exhibit remarkably similar SED shapes across samples (see [Figure 1](#)). In particular, the turnover wavelength (the characteristic “V-shaped” valley) remains narrowly confined around rest-frame  $\lambda \simeq 3000 - 4000 \text{ \AA}$  ([Setton et al. 2024](#)). This uniformity in the SEDs is difficult to reconcile with a scenario that requires variable contributions from two unrelated components. For instance, the explanation based on scattering processes would impose an almost universal distribution of dust and electrons in the nuclear region. More generally, any two-component model needs to explain the physical reason for maintaining a tight link between the emission sources, namely early coevolution between the central BH and young galaxy ([Inayoshi et al. 2025b](#)).

Moreover, dust reddening scenarios introduce a significant tension with independent infrared constraints. Dust obscuration necessarily implies dust heating and subsequent thermal re-emission in the mid- to far-infrared ([Barvainis 1987](#)). However, deep JWST/MIRI and ALMA observations show no significant detection of reprocessed IR flux in LRDs ([Williams et al. 2024](#); [Pérez-González et al. 2024](#); [Labbé et al. 2025](#); [Akins et al. 2025a](#); [Delvecchio et al. 2025](#); see also the stacked SED in [Figure 1](#)). The absence of IR emission excess challenges any interpretation that involves heavy obscuration.

### 2.3. Compact morphology

LRDs are selected as compact sources with angular sizes smaller than the point-spread function (PSF) of JWST/NIRCam imaging ([Barro et al. 2024](#); [Labbé et al. 2025](#)). Their inferred physical sizes are typically  $\lesssim 100 \text{ pc}$ , and the constraints reach down to  $\sim 10 - 30 \text{ pc}$  in gravitationally lensed cases. In most instances, LRDs show no clear signs of an extended host galaxy. Some LRDs have no detectable extended emission consistent with stellar emission ([Chen et al. 2025b](#)), where the tightest upper limits on stellar mass are derived based on realistic mock simulations. A significant fraction ( $\sim 30\% - 50\%$ ) of LRDs show spatially resolved, faint components in short-wavelength filters ([Killi et al. 2024](#); [Rinaldi et al. 2025](#)), but these are generally asymmetric and/or off-centered relative to the LRD position in longer-wavelength bands and are energetically subdominant ([Chen et al. 2025b](#)). Through analysis of 17 bands of NIRCam images, including a medium-band filter that captures  $[\text{O III}] \lambda 5007$ , at least one LRD shows extended, off-centered blue emission originating from nebular gas, not stars ([Chen et al. 2025a](#)). Image stacking analysis of  $\gtrsim 200$  LRDs observed in the COSMOS-Web survey also reveals extended components in four NIRCam bands, with the ratio of extended to total flux increasing toward shorter-wavelength filters (from 12% to 40%; [Zhang et al. 2025a](#)).

Additionally, LRDs are often found in non-isolated environments. High-resolution imaging frequently reveals nearby companions, either galaxies, nebular gas clumps, or even another V-shaped source (i.e., dual LRDs; see [Tanaka et al. 2024](#)). These companions may serve as potential reservoirs of gas and stars that can fuel or interact with the LRDs in subsequent evolutionary phases ([Chen et al. 2025a](#)). The build-up of their host-galaxy components may in fact drive the disappearance of LRDs toward lower redshifts, as the initially “naked” BHs lose their point-source characteristics and the characteristic V-shaped SED becomes less distinct ([Inayoshi 2025](#); [Billand et al. 2025](#); [Jones et al. 2025](#); [Mérida et al. 2025](#)). Nevertheless, the majority of LRDs are not hosted by well-established, massive galaxies; instead, their nuclear BHs appear to be overmassive relative to the local BH-to-galaxy mass correlation, although the BH mass estimates are still highly uncertain (see [Sections 5.1 and 5.2](#)).

## 2.4. Variability

Variability is a critical diagnostic for examining whether LRDs are powered by a single compact object or by a composite of multiple components. AGNs commonly exhibit intrinsic flux variability, reflecting changes in accretion rates or reprocessing on short timescales (e.g., Ulrich et al. 1997; Burke et al. 2021). Low-redshift highly accreting AGNs (e.g., narrow-line Seyfert 1 galaxies; NLSy1) are known to show rapid and low-amplitude (but nonzero) optical variability at the level of  $\sim 0.1$  mag (Du et al. 2016). Detecting such small variability requires high-precision flux calibration. In contrast, galaxies composed of many unsynchronized emitters (i.e., stars) typically show minimal coherent variability unless multiple stellar explosions occur within the observing time window.

To date, the JWST observational programs have not been originally designed for multi-epoch observations and make the detection of variability challenging. Kokubo & Harikane (2024) analyzed a small sample of high-redshift AGNs, including two LRDs, and found no significant variability above  $\gtrsim 0.1$  mag. Expanding on this, Zhang et al. (2025b) analyzed  $\sim 300$  publicly available LRD samples from multiple JWST surveys. They found that the majority of LRDs do not show detectable variability (see also Hayes et al. 2024 and Tee et al. 2025 using a combination of HST and JWST observational data), but identified eight LRDs showing clear flux changes of  $\gtrsim 0.3 - 0.8$  mag over timescales of  $\lesssim 10 - 100$  days in the observer’s frame. This result implies that the emission originates from compact regions with physical sizes of  $R \lesssim c\Delta t \lesssim 10^{-2}$  pc, much smaller than the PSF-limited image size of  $\lesssim 100$  pc.

One of the most intriguing LRDs for variability studies is Abell2744-QSO1, a triply gravitationally lensed source at  $z = 7.045$  (Furtak et al. 2024). Because the three lensed images correspond to path-length differences equivalent to a rest-frame baseline of  $\sim 2.5$  years, they allow us to probe intrinsic variability at three distinct epochs within a single set of observations. Two independent studies reported significant decreases in the equivalent widths (EWs) of H $\beta$  and H $\alpha$  emission lines (Ji et al. 2025a; Furtak et al. 2025), although it remains unclear whether these changes were caused by continuum brightening or emission-line fading due to uncertainties in flux calibration and lens modeling.

Some studies have argued that the apparent lack of variability may disfavor the AGN scenario. However, little or weak variability for LRDs is consistent with that of a subset of nearby AGN populations with stable UV fluxes (e.g., NLSy1 galaxies). Crucially, the detection of even a small but nonzero fraction of variable LRDs strongly supports the presence of compact, massive BHs at their centers.

## 2.5. Broad-line emission

A key observational signature of LRDs is the presence of broad hydrogen Balmer emission lines (H $\alpha$  and H $\beta$ ) with line widths of FWHM  $\gtrsim 1,000$  km s $^{-1}$ . These broad-line components are considered to originate from fast-moving gas clouds in the vicinity of a central massive BH (i.e., broad-line regions; BLRs), and to be a definitive characteristic of type 1 AGNs. Using empirical relations calibrated from nearby AGN populations, single-epoch spectroscopy of broad lines enables virial BH mass estimates (e.g., Greene & Ho 2005; Du et al. 2014). Although these estimates are subject to uncertainties due to uncertain dust extinction (Section 3.1) and possible additional broadening by electron scattering (Section 5.1), the typical BH masses lie in the range of  $M_{\text{BH}} \sim 10^6 - 10^7 M_{\odot}$  without extinction or scattering correction (Matthee et al. 2024; Maiolino et al. 2024; Lin et al. 2024; Taylor et al. 2025a; Kocevski et al. 2025).

Moreover, JWST-identified AGNs tend to exhibit systematically higher broad H $\alpha$  EWs (Maiolino et al. 2025a), approximately 3 times larger than those of low-redshift quasars (e.g., Vanden Berk et al. 2001; Greene & Ho 2005; Lusso et al. 2020). This difference suggests that the broad-line emission mechanisms in high-redshift faint AGNs may differ from those in nearby AGNs, for instance, through enhanced Balmer decrements in dense environments (see Section 2.6).

It is also worth noting that the color selection criteria based on the V-shaped SEDs and compact morphologies have proven highly effective in identifying LRDs with broad Balmer emission lines (Greene et al. 2024). A more systematic analysis by Hviding et al. (2025) using large spectroscopic data from the RUBIES survey found that LRDs selected based on rest-optical compact morphologies and V-shaped SEDs are likely ( $\gtrsim 80\%$ ) to have broad Balmer emission lines (the remaining 20% are not necessarily inconsistent with being broad-line AGNs). Other studies have reported that a similarly small fraction of photometrically selected LRD candidates show clear V-shaped spectra but with narrow H $\alpha$  emission (FWHM  $\simeq 200 - 300$  km s $^{-1}$ ) or with red colors dominated by strong narrow emission lines (Zhang et al. 2025c). Despite a small number of exceptions, these findings suggest a tight physical link between the three defining features of LRDs.

Alternatively, one might attempt to explain the broad  $H\alpha$  emission in LRDs through stellar phenomena, such as stellar winds or collections of supernova explosions (SNe). Wolf-Rayet (WR) galaxies characterized by young and massive stellar populations can indeed produce broad  $H\alpha$  emission (e.g., Ho et al. 1995; Schaerer et al. 1999). However, emission powered by hot, massive stars (WR stars and possibly interacting binaries) would also imprint characteristic spectral features, frequently associated with a He II  $\lambda 4686$  bump, which are not observed in LRDs. Moreover, reproducing the observed  $H\alpha$  luminosities of  $L_{H\alpha} \simeq 10^{41-42}$  erg s $^{-1}$  by multiple SNe would require an implausibly high rate of luminous transient events, implying extreme star formation rates at  $\gg 100 M_{\odot}$  yr $^{-1}$  (e.g., Kokubo & Harikane 2024; Maiolino et al. 2025a).

An additional possibility of non-AGN broad lines is that ultra-dense stellar clusters could produce broad emission via fast-moving gas clouds with velocities of  $\gtrsim 1,000$  km s $^{-1}$  (Baggen et al. 2024). However, this would require the stellar population to be confined within  $\sim 100$  pc scales, corresponding to an extraordinary stellar surface density of  $\Sigma_{\star} \simeq 10^{6-7} M_{\odot}$  pc $^{-2}$ , orders of magnitude higher than known star-forming system (see Section 3.2).

## 2.6. Balmer absorption, break, and decrement

LRD spectra show prominent absorption features superimposed on broad-line emission of hydrogen Balmer series and He I  $\lambda 10830$  in some cases (Matthee et al. 2024; Maiolino et al. 2024; Lin et al. 2024; Juodžbalis et al. 2024; Lin et al. 2024; Wang et al. 2025a; Kocevski et al. 2025; Inayoshi & Maiolino 2025; D'Eugenio et al. 2025). The detection of  $H\alpha$  and  $H\beta$  absorption is striking, as the  $n = 2$  excited state of atomic hydrogen is short-lived and not metastable. To produce visible absorption against broad Balmer emission, gas densities of  $n_H \gtrsim 10^{9-11}$  cm $^{-3}$  are required to populate the  $n = 2$  level via collisional excitation (Juodžbalis et al. 2024; Inayoshi & Maiolino 2025). We note that these required gas densities are comparable to those of BLR clouds observed in nearby AGNs (e.g., Kwan & Krolik 1981; Osterbrock & Ferland 2006). In the nearby universe, Balmer absorption is rare and seen in only  $\simeq 0.1\%$  of AGNs (e.g., Aoki et al. 2006; Shi et al. 2016; Schulze et al. 2018). In contrast, JWST observations have detected Balmer absorption in at least 10% – 20% of high-redshift broad-line AGNs (Matthee et al. 2024; Lin et al. 2024; Kocevski et al. 2025). Given that high-resolution spectroscopy is needed to identify such spectral features, the observed fraction is likely a lower limit (Maiolino et al. 2024), suggesting that many AGNs are enshrouded in dense gas covering a substantial solid angle.

Several LRDs observed with the low-resolution NIRSpec PRISM mode exhibit a characteristic bump near the Balmer limit wavelength of  $\lambda = 3646$  Å (Greene et al. 2024; Furtak et al. 2024; Labbé et al. 2024), separating the blue UV and red optical parts. This spectral feature superficially resembles a Balmer break from evolved stellar populations and has been interpreted as evidence of host galaxy contributions (Wang et al. 2024; Kokorev et al. 2024b; Akins et al. 2025a). If the light blueward of the Balmer break originates from a stellar source, stellar masses could be inferred as  $M_{\star} \sim 10^9 M_{\odot}$ , aligning with structure formation models (see Section 3.2). However, some LRDs exhibit a prominent Balmer break too deep to be explained by a stellar origin (Naidu et al. 2025; de Graaff et al. 2025; Taylor et al. 2025b). Importantly, such deep Balmer break features can be attributed to the same dense nuclear gas that produces Balmer absorption lines (Inayoshi & Maiolino 2025; Ji et al. 2025a; D'Eugenio et al. 2025). This process is analogous to the Lyman break, which results from neutral atomic hydrogen in the ground state ( $n = 1$ ) absorbing ionizing radiation.

Another key feature is the elevated Balmer decrement. The observed  $H\alpha/H\beta$  flux ratio often exceeds the values expected from either Case B recombination ( $\simeq 2.86$ ; Osterbrock 1974) or its partially optically thick variants ( $\simeq 3.05$ ; Osterbrock & Ferland 2006). While such higher ratios are commonly interpreted as the result of dust reddening (e.g. Mathis 1970, 1983; Calzetti et al. 1994; Dong et al. 2008), they may also arise from alternative processes (e.g., Baldwin 1975). In particular, collisional excitation and line trapping, where resonance scattering can divert  $H\beta$  photons to produce  $P\alpha\alpha$  and  $H\alpha$ , can enhance the Balmer line ratios without invoking significant dust attenuation (Krolik & McKee 1978; Kwan & Krolik 1981; Inayoshi et al. 2022c; Chang et al. 2025). The latter interpretation is supported by the observations of Balmer absorption imprinted on broad emission lines in many LRDs. These processes enhancing Balmer decrements in dense nuclear regions also align with significantly high EWs of broad  $H\alpha$  emission observed in JWST-identified AGNs (Section 2.5). Recently, Nikopoulos et al. (2025) extended spectral analysis to high-S/N sources by including additional Balmer lines such as  $H\gamma$  and  $H\delta$ , and found that high Balmer decrements both in  $H\alpha/H\beta$  and  $H\alpha/H\gamma$  appear consistent with dust reddening with  $A_V \simeq 3 - 5$  mag. However, such heavy extinction would contradict the weakness of hot dust emission in their spectra (see Section 2.7.2). Alternatively, dense broad-line emitting clouds with  $n_H \gtrsim 10^{10}$  cm $^{-3}$  can reproduce both the large Balmer decrement values and the  $H\alpha/H\beta$ - $H\alpha/H\gamma$  correlation.



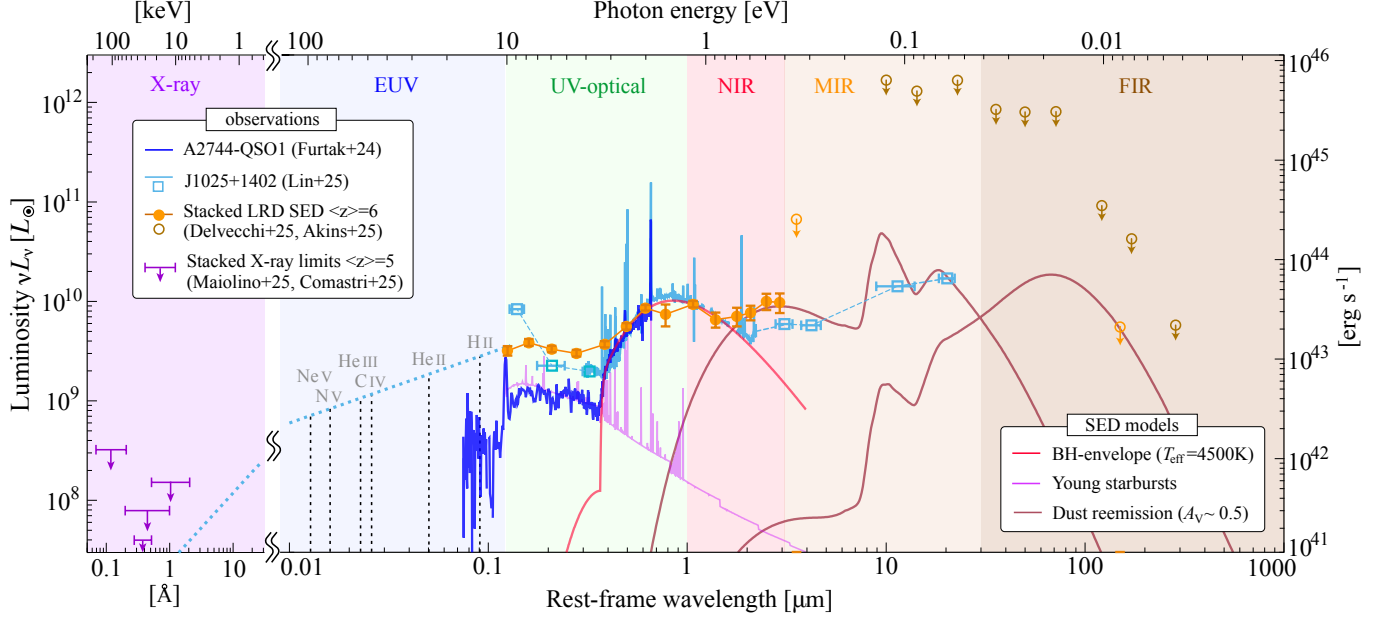


**Figure 1.** Multi-wavelength spectra of two representative LRDs: Abell2744-QSO1 at  $z = 7.045$  (blue, Furtak et al. 2024) and J1025+1402 at  $z = 0.1007$  with fluxes rescaled by a factor of 2.5 (cyan, Lin et al. 2025b). Rest-frame, median-stacked panchromatic SED based on publicly available data of JWST NIRCам, MIRI, and ALMA from the CEERS, GOODS-S, PRIMER-COSMOS, PRIMER-UDS surveys, as well as Spitzer and Herschel upper limits (detection/non-detection with filled/open circles, Akins et al. 2025a; Delvecchio et al. 2025). For comparison, the SED models of a BH-envelope with a surface temperature of  $T_{\text{eff}} = 4500$  K (red), a young starburst (magenta), and infrared reemission from heated dust with  $A_V \simeq 0.5$  mag (brown) are shown. The V-shaped SED in the enshrouded-BH scenario is taken from Inayoshi et al. (2025b) and the dust re-emission spectra are calculated to match either the MIRI detection or the deepest ALMA non-detection limit (Chen et al. 2025c). A power-law ionizing radiation spectrum with  $\alpha_{\text{ox}} = -1.7$  (dashed, Lusso et al. 2015) is overlaid with ionization energy thresholds for H, He, C, N, and Ne. The X-ray upper limits for JWST-identified AGNs in the Chandra Deep Field (Maiolino et al. 2025a; Comastri et al. 2025) are shown at the shortest-wavelength end of the spectrum, where the x-axis is compressed for visualization. The rest-frame 5 GHz upper limit (corresponding to a wavelength of 6 cm) is  $2 \times 10^{39} \text{ erg s}^{-1}$  (Mazzolari et al. 2024; Gloudemans et al. 2025), but this value lies far below the other luminosity constraints and thus falls outside the plot range optimized for the other wavelength data.

## 2.7. Constraints from other wavelengths

Multi-wavelength observational campaigns have been carried out to investigate the nature of LRDs, extending beyond the rest-frame UV-to-optical bands. In typical nearby AGNs, X-ray emission arises from hot plasma near the BH event horizon, near-infrared (NIR) emission is reprocessed by dust grains heated by AGN radiation, and radio synchrotron emission originates from relativistic jets and associated non-thermal processes. These spectral features are commonly used as diagnostics for AGNs when they are dust obscured, since high- and low-energy photons can penetrate dusty environments more effectively than optical and UV light (e.g., Ho 2008; Hickox & Alexander 2018). However, such canonical AGN signatures are largely absent or substantially weaker in LRDs.

### 2.7.1. X-ray weakness

X-ray observations are a key tool for identifying AGNs embedded in dense circumnuclear environments (Ueda et al. 2014; Aird et al. 2015; Nandra et al. 2015; Ricci et al. 2017; Ichikawa et al. 2019) due to the transmitted nature of high-energy photons. However, despite the presence of broad-line AGN signatures, most LRDs remain undetected even in deep Chandra X-ray data. Stacking analyses also yield no significant signal with an upper limit of  $L_{X,\text{obs}} < (2 - 4) \times 10^{41} \text{ erg s}^{-1}$  for JWST-identified AGNs (Yue et al. 2024a; Ananna et al. 2024; Maiolino et al. 2025a; Sacchi & Bogdán 2025; Comastri et al. 2025).

Hard X-rays are thought to originate from inverse Compton scattering of UV seed photons by hot nuclear plasma. Empirically, the absorption-corrected UV and X-ray luminosities of AGNs follow a tight correlation characterized by a spectral index between 2500 Å (or 4.96 eV) and 2 keV,  $\alpha_{\text{ox}} (\equiv d \log F_\nu / d \log \nu) \simeq -1.5$  to  $-1.8$  (e.g., Lusso

et al. 2015, see the dashed line in the EUV regime of Figure 1). Assuming that the observed UV luminosity ( $L_{\text{UV}} \simeq 1.5 \times 10^{43} \text{ erg s}^{-1}$ ) represents the intrinsic AGN power, the corresponding X-ray luminosity is expected to be  $L_X \simeq (1.3 - 8.0) \times 10^{41} \text{ erg s}^{-1}$ , broadly consistent with the current upper limits. Conversely, if the observed UV flux reflects only a small fraction of the intrinsic emission due to dust attenuation and scattering, the X-ray limits would suggest either intrinsic X-ray weakness ( $\alpha_{\text{ox}} \ll -1.8$ , significantly steeper than in normal AGNs) or the presence of Compton-thick absorbers with  $N_{\text{H}} > 10^{24} \text{ cm}^{-2}$ . The hydrogen column density is 2 orders of magnitude higher than expected from dust attenuation alone. Note that although the X-ray spectrum is heavily suppressed at  $E \lesssim 20 \text{ keV}$  for such Compton-thick cases ( $N_{\text{H}} \simeq 10^{24} \text{ cm}^{-2}$ ), the harder X-rays redshift into the observed  $2 - 10 \text{ keV}$  Chandra band for high-redshift objects, implying that even higher column densities would be required.

Intrinsic X-ray weakness is observed in nearby super-Eddington accretors (e.g., Wang et al. 2004; Dong et al. 2012; Laurenti et al. 2022; Tortosa et al. 2023), NLSy1 galaxies (Brandt et al. 2000; Liu et al. 2021), and AGNs with weak UV lines (Wu et al. 2012). Possible explanations include geometrically thick, super-Eddington accretion disks viewed at high inclination (Pacucci & Narayan 2024), efficient Compton cooling in funnel-like geometries (Madau & Haardt 2024), or cooling enhanced by mass-loaded disk winds (Inayoshi et al. 2025a). In any case, a tight upper limit from Sacchi & Bogdán (2025) suggests  $\dot{M}/\dot{M}_{\text{Edd}} \gtrsim 3$ , and the resulting soft X-ray spectra may also account for the weakness of UV emission lines in some LRDs (Lambrides et al. 2024).

### 2.7.2. $\Lambda$ -shaped Near-infrared SEDs

Infrared radiation emitted from hot dust irradiated by the LRD energy source provides key insights into their nuclear environments. In typical AGNs, compact dusty tori surround the central accretion disks with a finite covering fraction, reprocessing UV-optical radiation into the near- to mid-infrared (MIR) emission and producing characteristic IR excesses (e.g., Hönig & Kishimoto 2010). If LRDs hosted similar tori, hot dust near the sublimation temperature of  $T_{\text{dust}} \simeq 1500 \text{ K}$  would yield bright emission in the JWST/MIRI bands, naturally extending their red optical continua (e.g., Barvainis 1987). Despite extensive JWST/MIRI observations, however, most LRDs show no prominent IR excess (Williams et al. 2024; Pérez-González et al. 2024; Akins et al. 2025a), while a certain level of variations in NIR fluxes are reported among individual sources (Lyu et al. 2024).

Deep MIRI observations provide further constraints on the LRD properties when the IR spectral shape is well captured (Setton et al. 2025; Wang et al. 2025a). In these sources, the spectrum (in  $\nu L_\nu$ ) typically peaks at rest-frame  $\lesssim 1 \mu\text{m}$  and declines toward longer wavelengths with a slope of  $\beta_{\text{NIR}} < -1$ . The integrated NIR luminosity is comparable to or lower than the optical luminosity, and  $\simeq 2 - 3$  times higher than the UV luminosity. If the IR emission arises from reprocessed UV-optical radiation, energy conservation limits the dust extinction to  $A_V \lesssim 1 \text{ mag}$  and  $A_{\text{UV}} \lesssim 2 \text{ mag}$  (Chen et al. 2025c; see the SEDs in the MIR/FIR regimes of Figure 1). Steeper attenuation laws with  $A_{\text{UV}}/A_V > 3$  (e.g., the Small Magellanic Cloud or the Milky Way) yield even tighter limits on  $A_V \ll 1 \text{ mag}$ , which is too low to explain the red optical continuum by dust alone. Furthermore, the constraint on  $A_V$  suggests dust-poor or dust-free nuclear environments for LRDs and limits the dust mass to  $M_{\text{dust}} \lesssim 10^{4-6} M_\odot$  (Casey et al. 2025; Chen et al. 2025c). Assuming a dust production efficiency per stellar mass of  $f_{\text{dust},*} \sim 10^{-3}$  (Schneider & Maiolino 2024), the inferred low dust masses indicate only limited prior star formation, consistent with the absence of extended host galaxy features in JWST/NIRCam imaging (Chen et al. 2025b; see Section 2.3).

If LRDs are indeed dust-poor, what produces their red optical continua? Observationally, their optical-to-NIR spectra show “ $\Lambda$ ”-shaped SEDs characterized by steeply rising optical slopes and weak NIR emission ( $\beta_{\text{opt}} > 0$  and  $\beta_{\text{NIR}} < -1$ ). These spectra can be well reproduced by a single blackbody component with an effective temperature of  $T_{\text{eff}} \sim 5000 \text{ K}$ . While the physical origin of this thermal component remains uncertain (see Section 3.3), similar SED shapes have been observed in low-redshift LRDs whose rest-frame NIR-MIR spectra are available (Lin et al. 2025b; Ji et al. 2025b; see its spectral and photometric data in Figure 1), where the emission continues smoothly into the Rayleigh-Jeans tail with little hot-dust contribution. This characteristic thermal emission implies that BHs powering LRDs may be enshrouded within an optically thick gaseous layer under conditions reminiscent of red giant photospheres (Hayashi 1961).

### 2.7.3. Radio weakness

Radio observations are often used to trace jet activity or other radio-emitting processes of extragalactic sources. Deep radio data across a wide frequency range (144 MHz – 10 GHz) from the Very Large Array (VLA), Low-Frequency ARray (LOFAR), and MeerKAT for JWST-selected, spectroscopically confirmed broad-line AGNs reveal

no detections, placing a  $3\sigma$  upper limit at rest-frame 5 GHz of  $L_{5\text{GHz}} \simeq 2 \times 10^{39} \text{ erg s}^{-1}$  (Mazzolari et al. 2024; Gloudemans et al. 2025). This upper limit remains consistent with empirical  $L_X - L_{\text{H}\alpha}$  and  $L_X - L_{\text{R}}$  correlations established for local radio-quiet AGNs (e.g., Ho 1999; Ho & Peng 2001; Merloni et al. 2003; Saikia et al. 2015), as current radio observations are not yet deep enough to determine whether JWST-discovered AGNs are indeed radio weak. In this regime, the origin of any detected radio emission would show a wide range of morphologies, spectral shapes, and brightness temperatures, as is commonly observed among radio-quiet AGNs (Wang et al. 2023).

Deep ALMA observations have likewise failed to detect far-infrared emission expected from intense, dust-obscured star formation (Fujimoto et al. 2024), providing upper limits at ALMA bands (rest-frame  $100 - 300 \mu\text{m}$  for  $z \sim 6$  sources) of  $\nu L_\nu < 2 \times 10^9 L_\odot$  at ALMA 1.2 mm (e.g., Labbé et al. 2025; Xiao et al. 2025; Akins et al. 2025a; Setton et al. 2025; Casey et al. 2025; see the flux upper limits at longer wavelengths in Figure 1). These limits place strong constraints on stellar-origin scenarios, particularly implying dust mass below  $\lesssim 10^6 M_\odot$  (Casey et al. 2024, 2025), and suggest that star formation does not dominate the energetics of LRDs.

### 3. ORIGIN OF LRD POWER

Based on the observational characteristics summarized in Section 2, we investigate the physical origin of the energy source powering LRDs. We consider two possibilities: (1) gravitational energy released through mass accretion onto a massive BH and (2) nuclear energy from stellar activity, recalling the debates in the 1960-1970's regarding the power source of quasars (e.g., Salpeter 1964; Hoyle et al. 1964; Fowler 1964; Satō 1966; Lynden-Bell 1969; Lynden-Bell & Rees 1971). For each case, we examine whether the observed UV and optical energetics, the V-shaped SEDs, and the compact morphologies can be self-consistently explained without contradicting the other spectral characteristics (Sections 3.1 and 3.2, and Figure 2). In short, the AGN scenario provides a more natural explanation for the observed properties, but stellar components, *if any*, may still contribute to the UV emission.

We further discuss the gas-enshrouded AGN scenario, in which an accreting BH is enshrouded within optically thick, dense gas with a high covering fraction, as shown in the middle panel of Figure 2 (e.g., Inayoshi & Maiolino 2025; Kido et al. 2025; Liu et al. 2025; Naidu et al. 2025; de Graaff et al. 2025; Begelman & Dexter 2025; Rusakov et al. 2025). This configuration can be regarded as an extreme case of the AGN + dense gas scenario, where the medium surrounding the AGN forms a cocoon- or envelope-like structure. Such a configuration naturally accounts for several puzzling properties of LRDs.

#### 3.1. AGN scenario

In the AGN interpretation, the power source of LRDs is the gravitational energy released by material accreting onto a BH with mass of  $M$ . The radiation luminosity can be expressed by the product of the potential energy and mass accretion rate ( $\dot{M}$ ),

$$L \simeq \frac{GM\dot{M}}{r_0} \simeq \eta \dot{M} c^2, \quad (4)$$

where  $r_0$  is the energy dissipation radius. If  $r_0$  is set to the inner-most stable circular orbit, the radiative efficiency becomes  $\eta \simeq 0.1$  under the thin-disk approximation, where viscous heating is balanced with radiative cooling (Shakura & Sunyaev 1973; Novikov & Thorne 1973).

Let us begin with the optical energetics, which dominates the LRD power in the observed spectra. Here, we adopt a fiducial visual extinction of  $A_V \simeq 3 \text{ mag}$  to explain the red continuum color observed in LRDs (Kocevski et al. 2023; Matthee et al. 2024; Akins et al. 2025a), assuming that the intrinsic spectrum resembles composite, low-redshift AGN SEDs with optical slopes of  $-2 \lesssim \beta_{\text{opt}} \lesssim -1.5$  (Vanden Berk et al. 2001; Temple et al. 2021). Despite the uncertainties of  $A_V$  and extinction laws, the dust-corrected optical luminosity is on the order of  $L_{\text{opt}} \simeq 2 \times 10^{11} L_\odot$  (or  $\simeq 7 \times 10^{44} \text{ erg s}^{-1}$ ). The mass accretion rate required to produce the optical luminosity of LRDs is

$$\dot{M} = \frac{L_{\text{opt}}}{\eta c^2} \simeq 0.13 \eta_{0.1} M_\odot \text{ yr}^{-1} 10^{0.4(A_V-3)}, \quad (5)$$

where  $\eta_{0.1} = \eta/0.1$ .

The derived accretion rate corresponds to the Eddington accretion rate for a BH mass of  $M_{\text{BH}} \simeq 10^7 M_\odot$  at  $A_V = 3$ . Such inflow rates are achievable in protogalactic nuclei hosted by massive dark matter halos with masses of  $M_h$ , where



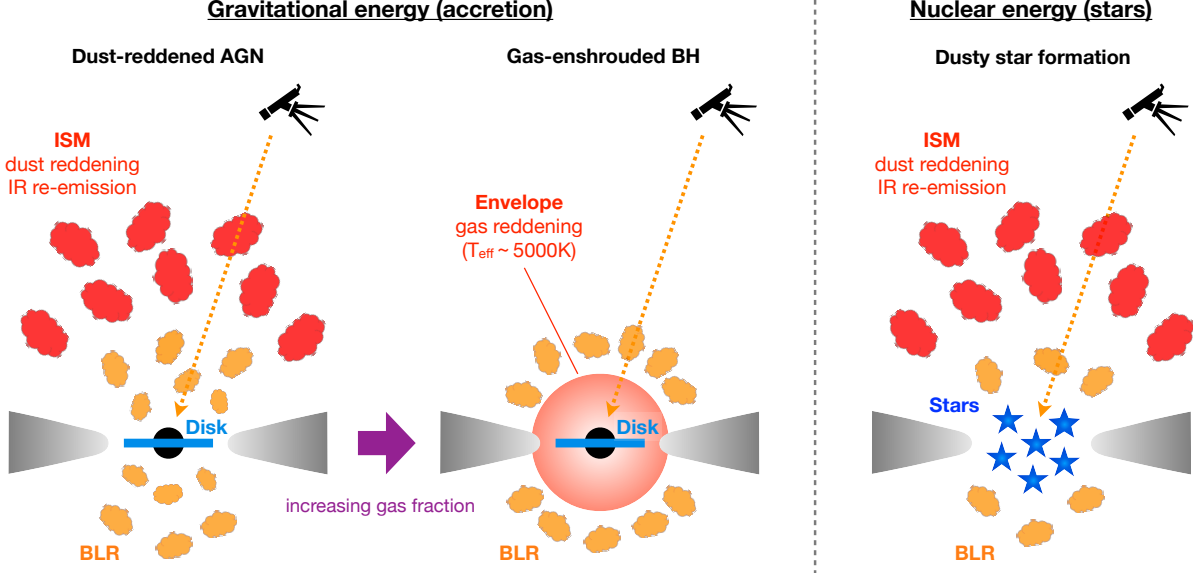


**Figure 2.** Summary of three proposed scenarios for the energy sources of LRDs. (1) **Dust-reddened AGNs:** broad-line AGNs with moderate dust extinction, explaining their red optical continua. (2) **Gas-enshrouded BHs:** AGNs embedded in dense gas with a high covering fraction, representing the extreme limit of an AGN + dense gas system. (3) **Dusty star formation:** systems where the red colors originate primarily from stellar emission attenuated by dust.

the baryonic inflow rate is given by

$$\dot{M}_b \simeq 15 M_\odot \text{ yr}^{-1} f_{b,0.16} \left( \frac{M_h}{10^{10} M_\odot} \right) \left( \frac{1+z}{10} \right)^{5/2}, \quad (6)$$

(e.g., Fakhouri et al. 2010; Dekel et al. 2013; see more detailed derivations in Inayoshi et al. 2025b), with the cosmic baryon fraction  $f_b (\equiv \Omega_b/\Omega_m) = 0.16$ ,  $f_{b,0.16}$ . Even if only a small fraction of the halo inflow reaches the nucleus (e.g.,  $\epsilon_{\text{nuc}} \sim 0.01 - 0.1$ ; Hopkins & Quataert 2010), the resulting accretion rate ( $\dot{M} = \epsilon_{\text{nuc}} \dot{M}_b$ ) is sufficient to power the optical energetics of LRDs consistently within the AGN framework.

However, explaining the UV emission of LRDs in the AGN scenario is not straightforward but requires fine-tuned conditions. The UV continuum emission of LRDs has a blue spectral slope of  $\beta_{\text{UV}} \simeq -2$ , consistent with that of unobscured quasars (Vanden Berk et al. 2001). This similarity suggests that the continuum shape either reflects the intrinsic AGN spectrum or is affected by minimal extinction, even though a large  $A_V$  value inferred from the red optical color leads to an inconsistent conclusion. To reproduce such UV emission by AGN radiation alone, only a few-percent of the intrinsic UV light must escape through small openings from the dusty obscuring region, if LRDs are truly obscured systems (Kocevski et al. 2023; Greene et al. 2024, as also discussed in Zakamska et al. 2005; Polletta et al. 2006). Although this may occur in individual cases, the observed uniformity of the V-shaped SEDs across the LRD population would require a fine-tuned efficiency of UV-photon scattering or escape. Otherwise, the turnover wavelength would vary significantly among sources, contrary to the observed narrow range around rest-frame  $\lambda \simeq 4000 \text{ \AA}$  (Setton et al. 2024).

An alternative possibility is that the UV light passes through a medium with an unusually flat extinction curve (i.e.,  $A_{\text{UV}} \simeq A_V$ ), as observed in composite AGN spectra (Gaskell et al. 2004), high-redshift star-forming galaxies (Markov et al. 2025), and the Orion Nebula (Baldwin et al. 1991), possibly due to a depletion of small dust grains with  $\lesssim 0.01 \text{ \mu m}$ . In such cases, the characteristic V-shaped SED would naturally arise from the shape of the dust attenuation curve itself rather than from stochastic scattering or leakage effects (Li et al. 2025d).

In any case, most of the UV emission (and the optical emission with  $A_V \simeq 3 \text{ mag}$ ) of AGNs is strongly attenuated by dust. As a result, the absorbed UV-optical radiation should be reprocessed as thermal infrared emission from heated dust (Chen et al. 2025c). However, JWST/MIRI observations have found faint rest-frame NIR luminosities significantly lower than the level expected from this scenario (Section 2.7.2).

### 3.2. Stellar scenario

We next consider the alternative possibility that the observed emission of LRDs originates from stellar processes within compact galaxies. As discussed below, this scenario may contribute to the UV part of the LRD spectrum, but faces problems when explaining the overall energetics and morphology.

In the stellar scenario, the observed optical luminosity can be reproduced by stars if the stellar mass is as high as

$$M_\star = \langle M_\star/L_V \rangle L_{\text{opt}} \simeq 1.6 \times 10^{11+0.4(A_V-3)} M_\odot, \quad (7)$$

where a typical mass-to-light ratio of  $\langle M_\star/L_V \rangle \simeq 0.1 M_\odot/L_{V,\odot}$  is adopted for young stellar populations (e.g., Bell & de Jong 2001; Into & Portinari 2013), and a visual extinction of  $A_V = 3$  mag is assumed to match the observed red optical continuum. Such a high stellar mass, comparable to or exceeding that of the Milky Way ( $M_{\star,\text{MW}} \simeq 5 \times 10^{10} M_\odot$ ), has also been derived from more sophisticated SED fitting for some LRDs at redshifts  $z \gtrsim 6-7$ , assuming that the optical emission originates from stars (Wang et al. 2024; Akins et al. 2025a). However, within the standard  $\Lambda$ CDM cosmology, such massive galaxies are expected to be exceedingly rare at these early epochs, and even if they exist, their formation would require an extremely high star formation efficiency of  $\epsilon_\star \gtrsim 30-100\%$  (e.g., Inayoshi et al. 2022a; Boylan-Kolchin 2023; Dekel et al. 2023). Furthermore, the compact morphology of LRDs imposes a severe additional constraint. The entire stellar population must be confined within  $\sim 100$  pc, yielding an extraordinarily high stellar surface density of  $\Sigma_\star \simeq 10^{6-7} M_\odot \text{ pc}^{-2}$  (Baggen et al. 2024). These densities exceed those of even the densest stellar systems known in the nearby universe (e.g., nuclear star clusters with  $\Sigma_\star \simeq 10^5 M_\odot \text{ pc}^{-2}$ ; Hopkins et al. 2010), and would likely lead to dynamical instabilities and gravitational collapse on timescales of  $\lesssim 1$  Myr (Pacucci et al. 2025).

The inferred stellar mass can be lowered by more than an order of magnitude if only the UV and 4000 Å break features (excluding the red optical continua) are attributed to evolved stellar populations under negligible dust extinction. In this case, the 4000 Å break can be explained by  $\gtrsim 0.5-1.0$  Gyr-old stars (i.e., stellar Balmer break) that dominate the low-mass end of the initial mass function, requiring a total stellar mass of  $M_\star \sim 10^{9-10} M_\odot$  and a star formation rate of  $\text{SFR} \sim 1-10 M_\odot \text{ yr}^{-1}$  (e.g., Wang et al. 2024). Although this scenario eases the tension with cosmological abundance and density limits, such systems would still lie near the upper limits plausible at these redshifts.

If only the UV continuum (blueward of the 4000 Å break) originates from stellar emission, the required conditions become much less stringent. In this case, young massive stars from ongoing star formation can reproduce the observed blue UV continuum at

$$\text{SFR} = \mathcal{K}_{\text{UV}} L_{\text{UV}} = 1.0 M_\odot \text{ yr}^{-1} \left( \frac{\mathcal{K}_{\text{UV}}}{10^{-10} M_\odot \text{ yr}^{-1} L_\odot^{-1}} \right) \left( \frac{L_{\text{UV}}}{10^{10} L_\odot} \right), \quad (8)$$

where the conversion factor  $\mathcal{K}_{\text{UV}}$  depends on the stellar initial mass function, metallicity, and stellar age (Madau & Dickinson 2014; Zackrisson et al. 2011; Harikane et al. 2024). Adopting the fiducial conversion factor, the UV luminosity becomes as high as  $L_{\text{UV}} \simeq 10^{10} L_\odot$ , comparable to typical UV luminosities (uncorrected for dust) of observed LRDs. With an age of  $\sim 10$  Myr, the stellar mass of the young stellar cluster is  $M_\star \sim 10^7 M_\odot$ . Assuming Case B radiative recombination for atomic hydrogen, the  $\text{H}\alpha$  luminosity can be estimated as  $L_{\text{H}\alpha} = 6.9 \times 10^{41} \text{ erg s}^{-1} (\text{SFR}/1 M_\odot \text{ yr}^{-1})$ , where the conversion factor is based on a  $Z_\odot/50$  stellar population (Schaerer 2002).

### 3.3. Enshrouded AGN scenario

As discussed above, the AGN scenario is plausible in energetics but has a difficulty in explaining the IR weakness if the optical red continuum is shaped by dust extinction. To solve this problem, and also motivated by the presence of dense circumnuclear gas implied by Balmer absorption, Balmer break, and Balmer decrement, an alternative picture has been proposed in which an accreting BH is deeply embedded in a dense gaseous environment. This configuration can be regarded as an extreme case of the AGN + dense-gas scenario, in which the surrounding medium forms a cocoon-like distribution (the middle panel of Figure 2).

In such a setup, the BH is enshrouded by an optically thick, extended gaseous structure. The obscuring medium may take the form of a quasi-hydrostatic envelope or a clumpy, geometrically thick gas distribution supported by the central BH engine. Regardless of the detailed geometry and origin, such configurations naturally produce a relatively cool effective temperature of  $T_{\text{eff}} \simeq 4000-6000$  K. This temperature range corresponds to the minimum value attainable in an optically thick, partially ionized gas where  $\text{H}^-$  opacity dominates. This narrow temperature range defines the

so-called Hayashi line observed as a nearly vertical track on the Hertzsprung-Russell diagram for cool, fully convective stellar envelopes (Hayashi 1961; Hayashi et al. 1962), although this analogy applied to LRDs does not require the gas to be in a strictly stellar-like envelope.

With this interpretation, the red optical continua of LRDs can be understood as the Wien tail of a blackbody spectrum with  $T_{\text{eff}} \simeq 5000$  K without relying on dust reddening (Inayoshi et al. 2025b,c; Kido et al. 2025; Liu et al. 2025; Begelman & Dexter 2025), and this emission spectral shape also explains the weak IR emission (Casey et al. 2024, 2025; Li et al. 2025d; Setton et al. 2025; Chen et al. 2025c). Indeed, blackbody-like emission emerging from optically thick, dust-poor dense gas provides a more natural explanation for LRDs with strong Balmer breaks and clear  $\Lambda$ -shaped SEDs in the rest-frame optical and NIR regime (Labbé et al. 2024; Naidu et al. 2025; de Graaff et al. 2025; Taylor et al. 2025b). Moreover, the dense gaseous structure accounts for the absence of X-rays due to high Compton thickness, and plausibly also the lack of radio emission expected from AGN jets owing to effective jet energy dissipation into the surrounding dense medium.

Such dense gaseous structures can be supported in several physical contexts. They may arise around BHs accreting at super-Eddington rates, where radiation pressure inflates the surrounding gas into an extended envelope (Inayoshi et al. 2016; Takeo et al. 2020; Shi et al. 2023). Similar structures are also expected in quasi-stars (Begelman et al. 2006, 2008; Volonteri & Begelman 2010; Coughlin & Begelman 2024) and in the brief stellar-like phase of supermassive stars formed along the direct-collapse BH pathway (Hosokawa et al. 2013; Woods et al. 2021; Mayer et al. 2024). Under the conditions where radiative energy losses become inefficient due to high optical depths, the bloated gas resembles convection-dominated accretion flows (Quataert & Gruzinov 2000), in which inflows and outflows coexist. Convective eddies reduce the inward mass flux toward smaller radii, following a power-law form of  $\dot{M}_{\text{in}} \propto r^p$ , with  $p \simeq 0.5 - 0.7$  observed in numerical simulations (e.g., Stone et al. 1999; Yuan & Narayan 2014). As a result, even if the large-scale mass inflow rate greatly exceeds the Eddington value, the BH feeding rate self-regulates to  $\dot{M}_{\text{BH}} \sim \mathcal{O}(\dot{M}_{\text{Edd}})$  (e.g., Hu et al. 2022), and the emergent luminosity remains near  $L_{\text{ph}} \simeq L_{\text{Edd}}$ .

Assuming that the photospheric luminosity is close to the Eddington luminosity ( $\lambda_{\text{Edd}} \equiv L_{\text{ph}}/L_{\text{Edd}} \simeq 1$ ), the BH mass is directly inferred as

$$M_{\text{BH}} \simeq 3 \times 10^6 M_{\odot} \lambda_{\text{Edd}}^{-1} \left( \frac{L_{\text{ph}}}{10^{11} L_{\odot}} \right). \quad (9)$$

The outer boundary of the obscuring gas, where the emergent continuum becomes optically thin, defines a photospheric radius

$$R_{\text{ph}} = \sqrt{\frac{L_{\text{ph}}}{4\pi\sigma_{\text{SB}}T_{\text{eff}}^4}} \simeq 1.7 \times 10^{16} \text{ cm } \lambda_{\text{Edd}}^{1/2} M_6^{1/2} T_0^{-2}, \quad (10)$$

where  $M_6 = M_{\text{BH}}/(10^6 M_{\odot})$ ,  $T_0 = T_{\text{eff}}/(5000 \text{ K})$ , and  $\sigma_{\text{SB}}$  is the Stefan-Boltzmann constant. The circular velocity associated with the gravitational potential at this radius is

$$V_{\text{ph}} = \sqrt{\frac{GM_{\text{BH}}}{R_{\text{ph}}}} \simeq 3.0 \times 10^{-3} c \lambda_{\text{Edd}}^{-1/4} M_6^{1/4} T_0, \quad (11)$$

where  $G$  is the gravitational constant and  $c$  is the speed of light. This characteristic radius is comparable to the typical BLR scale measured from reverberation mapping in normal AGNs (e.g., Kaspi et al. 2000; Bentz et al. 2009). Gas orbiting near this radius naturally produces emission-line widths of order of  $\mathcal{O}(V_{\text{ph}})$ . Moderate electron scattering in the slightly deeper, optically thick layers adds an additional broadening component and yields the observed exponential line profiles (Rusakov et al. 2025).

Although the BH-envelope (more generally gas-enshrouded AGNs) framework provides a self-consistent explanation for many key properties of LRDs, it also faces a challenge in accounting for the origin of the UV continuum and the broad-line emission. A cool, optically thick gas with  $T_{\text{eff}} \simeq 5000$  K cannot generate a strong UV continuum or produce ionizing photons. Moreover, high-energy radiation emitted by the central accretion disk is unlikely to escape through such dense media. Even if a fraction of the UV/ionizing photons emerges through low-density polar channels or within a clumpy medium, the resulting SED would depend sensitively on the viewing angle and the distribution of the clumpy gas, making it difficult to maintain the spectral uniformity among LRDs. An alternative is that the UV continuum may originate from outside the envelope, for instance, from a compact nuclear star-forming region surrounding the accreting BH. While such an additional UV source can reproduce the observed UV spectra and thus the overall V-shaped SEDs, achieving this also requires either fine-tuning the luminosity ratio between the stellar component and the

	AGN	Enshrouded AGN	Galaxy	Notes
Image	✓ BHs		✗ Compact galaxies	No obvious host galaxies in most LRDs. Extremely high stellar density if all emission is from stars.
Broad-line emission	✓ Broad-line regions		? WRs/SNe	In stellar scenarios, some stellar activity (WR winds and SNe) or a very deep stellar potential could yield broad lines, but each case has some issues (see text).
Variability	✓ Weak/non-zero variability		✗ No variability	Super-Eddington accretion exhibits weak variability, consistent with most LRDs. Some LRDs with clear variability contradict the stellar scenario.
Balmer break & absorption	✓ Dense gaseous absorbers	✓ Gas envelopes	✗ Evolved galaxies	Absorption on stellar continua is too weak to imprint absorption on top of broad-line emission. Some LRDs exhibit breaks too deep to be consistent with starlight.
Blue UV	? Scattered light of AGN	? Clumpy absorbers/ Additional stars	✓ Unobscured galaxy	The uniformity of V-shaped SEDs requires a fine-tuning of the relative contribution. UV part can be explained by reasonable stellar mass and SFR.
Red optical	✗ Dust-reddened AGN	✓ Optically thick gaseous envelope	✗ Dusty star formation	The stellar mass required in the galaxy scenario is too massive to form in high-redshift halos.
Faint NIR	✗ Hot dust	✓ Thermal spectrum from gaseous envelope	✓ Stellar spectrum	Bright NIR in dust-reddened AGN violates MIRI. A gaseous envelope naturally explains flat IR spectrum.
X-ray weak	✓ Super-Eddington/ Compton thickness		✓ Intrinsically weak	Corona cools down in super-Eddington accretion flows with outflows and funnel-like density structures.
Radio weak	✓ Radio-quiet AGN		✓ Intrinsically weak	Radio non-detection of LRDs is consistent with current detection limits for radio-quiet AGNs.
ALMA weak	✓ Consistent		✗ Cold dust emission	ALMA constraints limit dust mass. Star formation does not dominate LRD energy.

**Figure 3.** Summary of the key observed properties of LRDs and their physical interpretations under the AGN, enshrouded AGN, and galaxy scenarios. Each feature is classified as favorable (✓), unfavorable (✗), or uncertain (?) for each model with short notes explaining the rationale. Most observed characteristics are best explained by accreting-BH models, particularly the enshrouded-AGN framework, whereas the galaxy hypothesis requires extreme fine-tuning and remains inconsistent with several constraints.

gas-attenuated AGN (Wang et al. 2024; Kocevski et al. 2025; Ma et al. 2025a) or a physical mechanism that naturally regulates it. Recently, Inayoshi et al. (2025b) proposed that gas inflows during the assembly of massive halos with  $M_h \gtrsim 10^{11} M_\odot$  at  $z \sim 4 - 7$  trigger simultaneous BH feeding and nuclear starbursts, whose synchronized coevolution through feedback naturally drives the luminosity and mass ratios between the two components to converge toward the values inferred from LRD observations. Cumulative injection of energy and momentum by SNe subsequently expels gas from the nucleus, quenches gas supply to the BH envelope, and ultimately leads to a transition into normal AGN phases.

### 3.4. Summary table

In Figure 3, we summarize how key observational features of LRDs are interpreted under the AGN and galaxy hypotheses, including the gas-enshrouded AGN scenario. Each feature is classified as favorable (✓), unfavorable (✗), or uncertain (?) for each model. Many observed properties, such as the compact morphology, broad Balmer emission, red optical continua, and ALMA non-detections, are naturally explained by accreting BH scenarios. Balmer absorption and red optical continua can arise from dense, optically thick envelopes associated with super-Eddington accretion, which simultaneously accounts for the weakness of X-rays and variability. Importantly, thermal emission from such envelopes reproduces weak NIR spectra, in contrast to dust-reddened AGN interpretations.

The galaxy hypothesis, on the other hand, struggles to reproduce the lack of host signatures and the broad-line spectra without invoking unrealistically dense or massive stellar systems. ALMA non-detections place a stringent limit on the SFR and dust content in LRDs.

Overall, the collective evidence favors an AGN origin, with the enshrouded AGN framework providing the most self-consistent explanation of the multi-wavelength properties of LRDs.

## 4. COSMOLOGICAL EVOLUTION

### 4.1. Cosmic abundance

Since their discovery, more than 500 photometrically selected LRDs have been reported, and  $\sim 10\%$  of them have been spectroscopically confirmed as broad-line AGNs (e.g., [Matthee et al. 2024](#); [Greene et al. 2024](#); [Hainline et al. 2025](#); [Kocevski et al. 2025](#)). The majority of the remaining sources are also likely broad-line AGNs, given that LRDs selected with V-shaped SEDs and compact morphologies show a high spectroscopic confirmation rate ( $\gtrsim 80\%$ ) for broad-line AGNs ([Hviding et al. 2025](#)). The large number of LRDs identified within narrow fields of view in JWST programs suggests that their cosmic abundance reaches  $\phi_{\text{LRD}} \simeq 10^{-6} - 10^{-4} \text{ Mpc}^{-3}$  over  $-21 \lesssim M_{\text{UV}} \lesssim -17$  at  $z \sim 4 - 9$  (e.g., [Kokorev et al. 2024a](#); [Kocevski et al. 2025](#); [Akins et al. 2025a](#)), corresponding to  $\sim 1\%$  of the galaxy abundance at the same brightness (e.g., [Finkelstein et al. 2015](#); [Bouwens et al. 2021](#); [Harikane et al. 2022](#)).

Due to the nature of their color selection, LRDs are primarily identified at  $z \sim 4 - 9$ , where JWST multi-band filters can simultaneously capture both the blue UV and red optical continua. The most distant confirmed LRD to date is CAPERS-LRD-z9 at  $z = 9.3$  ([Taylor et al. 2025b](#)), which was identified directly from its spectroscopic features of a V-shaped SED, a prominent Balmer break, and broad  $\text{H}\beta$  emission with  $\text{FWHM} = 3,500 \text{ km s}^{-1}$ , corresponding to a single-epoch BH mass of  $M_{\text{BH}} \simeq 4 \times 10^7 M_{\odot}$ . At even higher redshifts ( $z \gtrsim 10$ ), characterizing the red optical continuum requires MIRI photometry, which is generally shallower than NIRCам data and thus biases detections toward intrinsically brighter objects. [Tanaka et al. \(2025\)](#) have presented the first search for LRDs at  $z \gtrsim 10$  using both NIRCам and MIRI F770W imaging in the COSMOS-Web field.

On the other hand, identifying LRDs at lower redshifts ( $z \lesssim 3$ ) is also challenging. At these redshifts, the blue UV component and the Lyman break cannot be fully captured with JWST alone, and potential contamination from dusty red galaxies increases. Therefore, reliable source identification requires complementary datasets from the Hubble Space Telescope and ground-based facilities such as the Subaru Telescope. As a result, several photometric LRD candidates have been reported at  $z \sim 2 - 3$ , yielding an estimated abundance of  $\sim 10^{-6} \text{ Mpc}^{-3}$  ([Ma et al. 2025b](#); [Euclid Collaboration et al. 2025](#); [Zhuang et al. 2025](#)), which is approximately 2 orders of magnitude lower than that at  $z \sim 4 - 9$ . However, since none of these intermediate-redshift candidates have yet been spectroscopically confirmed as AGNs, this abundance should be regarded as an upper limit.

The redshift evolution of the LRD abundance shows a distinct trend compared to that of normal AGNs: the number density increases from  $z \gtrsim 8$ , peaks at  $z \sim 6 - 7$ , and then declines rapidly toward lower redshifts ([Kocevski et al. 2025](#)). [Inayoshi \(2025\)](#) found that this evolution is well described by a log-normal distribution, commonly associated with phenomena driven by stochastic processes, and proposed a hypothesis that LRDs represent the earliest one or two accretion episodes of newly formed BH seeds. These initial episodes exhibit characteristic spectral signatures (e.g., V-shaped SEDs) that fade during subsequent accretion phases. The redshift-dependent comoving number density of LRDs is modeled in [Inayoshi \(2025\)](#) as

$$\phi_{\text{LRD}} = \phi_0 f(z) \exp \left[ -\frac{\{\ln(1+z) - \mu_z\}^2}{2\sigma_z^2} \right], \quad (12)$$

where  $\log(\phi_0/\text{Mpc}^{-3}) = -5.27 \pm 0.0015$ ,  $\mu_z = \ln(1+z_0)$  with a characteristic redshift of  $z_0 (= 6.53^{+0.04}_{-0.03})$  corresponding to the cosmic age  $t_0 (= 837 \pm 6 \text{ Myr})$ , and  $\sigma_z = 0.218 \pm 0.00535$ . The function  $f(z)$  accounts for the redshift dependence of both the comoving volume and cosmic time interval, and is approximated as

$$f(z) = \frac{(1+z)^{3/2}}{[s(1+z)^{1/2} - 1]^2}, \quad (13)$$

and  $s = 0.903$  is fitted for a flat  $\Lambda$ CDM universe with  $\Omega_{\text{m}} = 0.307$  at  $z \geq 1.5$ . This analytical form provides a simple model for the evolution of the LRD population, which can be readily extended to luminosity function studies and tested with future JWST surveys, particularly at low and high redshifts (see [Ma et al. 2025b](#)).



#### 4.2. Soltan-Paczynski argument

The high cosmic abundance of LRDs reveals that they are not rare but instead dominate the AGN population at high redshifts. In the early stage of LRD studies, one generally interpreted LRDs as dust-reddened AGNs with moderate extinction ( $A_V \sim 3$  mag). Using the extinction-corrected LRD luminosity function, Inayoshi & Ichikawa (2024) and Akins et al. (2025a) found that the BH accretion rate density does not decline but instead rises toward higher redshifts ( $z \gtrsim 6$ ), exceeding the value inferred from X-ray and infrared AGN surveys (e.g., Ueda et al. 2014; Delvecchio et al. 2014; Aird et al. 2015; Ananna et al. 2019; Pouliazis et al. 2024). This counterintuitive trend becomes even pronounced when the bright-end populations from the COSMOS-Web survey are included in the analysis (Akins et al. 2025a).

The cumulative mass density of BHs during LRD phases inferred from the radiative output with an assumed radiative efficiency should align with the remnant BH mass density at subsequent epochs (neglecting mass loss by gravitational wave emission led by mergers). For typical AGNs with X-ray detection at  $0 < z < 5$ , comparison with the BH mass density at  $z = 0$  yields a robust constraint of  $\eta \simeq 0.1$  (e.g., Soltan 1982; Yu & Tremaine 2002), consistent with the canonical value for a geometrically thin accretion disk (Shakura & Sunyaev 1973; Novikov & Thorne 1973). In contrast, reproducing the observed BH mass density at  $z \sim 4 - 5$  from the accretion implied by the LRD luminosity functions requires a radiative efficiency at least twice as high ( $> 3\sigma$  significance), implying that these BHs rapidly spin up to  $\gtrsim 96\%$  of the maximum limit. Improved estimates of BH mass and luminosity for LRD populations will refine the constraints on radiative efficiencies and associated spins (see Sections 3.3 and 5.1).

#### 4.3. Local LRD analog

Although LRDs are predominantly found at high redshifts, several LRD-like objects have been reported in the nearby universe ( $z \sim 0.1 - 0.2$ ) (Lin et al. 2025a,b; Ji et al. 2025b). These sources exhibit hallmark LRD features: (1) a V-shaped UV-optical SED, (2) compact morphology, (3) broad Balmer/Paschen and He I emission (FWHM  $\simeq 1000 - 2000$  km s $^{-1}$ ) with narrow absorption, (4) weak NIR fluxes, (5) X-ray weakness, and (6) no significant variability. Lin et al. (2025a) showed that some local “green pea” galaxies, which are classified as compact dwarf galaxies, share several key properties with high-redshift LRDs, including V-shaped SEDs, broad Balmer emission, and BH overmassiveness relative to the local scaling relation. For three additional, low-redshift LRD-like sources (Lin et al. 2025b; Ji et al. 2025b), high-resolution spectra covering rest-frame optical to NIR enable detailed studies of their continua and line properties, which are inaccessible to JWST/NIRSpec (and only marginally probed by MIRI photometry). WISE data further constrain their MIR emission and reveal that the optical-NIR continuum emission is well reproduced by a blackbody with  $T_{\text{eff}} \simeq 5000$  K, including a Balmer break imprint consistent with radiative transfer effects (Liu et al. 2025). This agrees remarkably well with the predictions from the BH-envelope model (Inayoshi et al. 2025b,c; Kido et al. 2025; Begelman & Dexter 2025; Nandal & Loeb 2025).

One striking example, J1025+1402 (“The Egg”), shows extremely strong Na D, K I, Fe II, and Ca II triplet absorption, further supporting the presence of a cool, metal-enriched gas envelope. These features as well as the optical continuum spectrum resemble those of G-to-K giant stars (even a G-band molecular absorption produced under extremely high gas densities of  $n_{\text{H}} \gtrsim 10^{14}$  cm $^{-3}$ ). Furthermore, this object exhibits a series of optical [Fe II] emission lines indicative of low-ionization, dense gas with  $n_{\text{H}} \gtrsim 10^6$  cm $^{-3}$  between broad and narrow-line regions (Lin et al. 2025b; Ji et al. 2025b; Torralba et al. 2025a).

Such nearby LRD analogs offer unique laboratories to probe the physical structure and kinematics of the gas in the LRD interior. Future high-resolution spectroscopic studies will be crucial to test whether the broad-line region originates from a stratified, multi-phase envelope and to quantify the escaping efficiency of ionizing and UV photons from these systems.

### 5. DISCUSSION

#### 5.1. BH mass estimators

The key advantage of broad-line AGNs is that their BH masses can be estimated from a single-epoch virial relation,  $M_{\text{BH}} \propto (\text{FWHM})^2 \cdot R_{\text{BLR}} \propto (\text{FWHM})^2 \cdot L^{1/2}$ . Applying this technique to LRDs with broad Balmer emission yields typical masses of  $M_{\text{BH}} \simeq 10^{6-8} M_{\odot}$ . However, this calibration is based on local, unobscured broad-line AGNs where the continuum and line emissions are tightly correlated (Greene & Ho 2005). Moreover, single-epoch mass estimates for super-Eddington cases would be biased toward high values (e.g., Du et al. 2014; Lupi et al. 2024b). Most LRD

studies have assumed moderate dust extinction ( $A_V \sim 3$  mag) inferred from the red continuum slope and, if available, the Balmer decrement. With extinction correction applied to the line or continuum luminosities, the inferred BH masses increase by a factor of  $\simeq 10^{0.2A_V}$ . Yet, such reddening would produce bright NIR emission inconsistent with the observed JWST/MIRI data, which imply  $A_V \ll 1$  mag (Chen et al. 2025c). If this is the case, the true BH masses are likely overestimated by a factor of  $\sim 3 - 4$  in previous studies that assume  $A_V \sim 3$  mag.

Intriguingly, a significant fraction of high-S/N LRD spectra show broad-line emission profiles better described by an exponential rather than a single Gaussian function (Rusakov et al. 2025). This behavior suggests that scattering by free electrons with thermal velocity  $v_{\text{th,e}} = \sqrt{2k_B T/m_e} \simeq 550 \text{ km s}^{-1}$  for  $T = 10^4 \text{ K}$  may shape the line wings (see also Laor 2006; Chang et al. 2025). Such scattering broadens the emission lines without altering their intrinsic kinematics, implying that the observed FWHM values are likely overestimated relative to their true widths. As a result, BH masses derived from single-epoch virial estimators could be overestimated by up to 2 orders of magnitude in some cases (Rusakov et al. 2025), although a double-Gaussian fit can reproduce the line profiles comparably well (Juodžbalis et al. 2025a). A caveat is that electron scattering is elastic (i.e., photon energies are conserved) and thus observed luminosities remain unaffected. Therefore, one must still account for the observed luminosities of the broad H $\alpha$  line and the optical continuum emission ( $\sim 10^{43-44} \text{ erg s}^{-1}$ ) in the energy budget. From this energetics requirement (see Section 3.1), the BH mass cannot be arbitrarily reduced but the number of electron scatterings is likely limited to only one to a few (Rusakov et al. 2025; Chang et al. 2025). Indeed, an independent, direct dynamical BH mass measurement based on the H $\alpha$  line kinematics for Abell2744-QSO1 is consistent with the single-epoch virial estimate instead of the scattering-modified case (Juodžbalis et al. 2025b).

Finally, we comment on the BH mass estimate in the enshrouded-AGN model. In this scenario, owing to the blackbody nature of the spectrum and envelope-regulated accretion, the photospheric luminosity is expected to be on the order of  $\sim \mathcal{O}(L_{\text{Edd}})$ , yielding a BH mass of  $M_{\text{BH}} \simeq 3 \times 10^6 M_{\odot} \lambda_{\text{Edd}}^{-1} (L_{\text{ph}}/10^{11} L_{\odot})$  (Equation 9). Under the blackbody assumption, the bolometric correction from rest-frame 5100 Å is  $f_{\text{bol}} \simeq 1.8$ , significantly lower than the typical AGN value ( $f_{\text{bol}} \simeq 9.26$ ; Richards et al. 2006). A similarly modest correction of  $f_{\text{bol}} \simeq 5.0$  is calculated by Greene et al. (2025), based on the observed multi-wavelength spectra of A2744-45924 (Labbé et al. 2024) and RUBIES-BLAGN-1 (Wang et al. 2025a).

## 5.2. The $M_{\text{BH}}-M_{\star}$ relation

In the present-day universe, a tight correlation has been observed between SMBH masses and host galaxy properties (e.g., bulge mass and stellar velocity dispersion; see reviews in Kormendy & Ho 2013 and Greene et al. 2020), suggesting that SMBHs and galaxies have coevolved through feeding and feedback over cosmic time. A fundamental open question is how and when this BH-galaxy relation was first established. In this context, newly identified LRDs provide a valuable clue: their inferred BH-to-galaxy mass ratios are significantly higher than those in the local universe, as their host galaxies remain poorly detected, if at all, in both imaging and spectroscopy (e.g., Maiolino et al. 2024; Lin et al. 2024; Furtak et al. 2024; Wang et al. 2024; Labbé et al. 2024, 2025; Kocevski et al. 2025; Chen et al. 2025b,a, see also Kokorev et al. 2024b; Li et al. 2025a). These findings suggest that LRDs host initially overmassive BH seeds and/or experience rapid super-Eddington accretion in the early universe.

For comparison, although traditionally quasar host galaxies have also been challenging to detect under the overwhelming glare of the AGN, JWST observations have yielded better success in separating the AGN from the host, especially in low-luminosity quasars (e.g., Ding et al. 2023, 2025; Stone et al. 2024; Yue et al. 2024b), but also in more powerful sources with the advent of improved decomposition techniques (Li et al. 2025c). Since LRDs are several orders of magnitude fainter than luminous quasars, they offer a promising opportunity to detect the underlying stellar emission. Nevertheless, even with JWST/NIRCam, their host galaxies, if any, remain unresolved. The inferred upper limit on their effective radius ( $\lesssim 100 \text{ pc}$ ) implies a stellar mass of  $M_{\star} \lesssim 10^9 M_{\odot}$  (e.g., Chen et al. 2025b,a). Combining this stellar mass with single-epoch virial BH mass estimates yields  $M_{\text{BH}}/M_{\star} \gtrsim 0.01 - 0.1$  (e.g., Kocevski et al. 2023; Pacucci et al. 2023; Maiolino et al. 2024; Lin et al. 2024; Furtak et al. 2024; Kocevski et al. 2025; Jones et al. 2025), significantly above the local  $M_{\text{BH}} - M_{\star}$  relation (e.g., Kormendy & Ho 2013; Greene et al. 2020; Zhuang & Ho 2023).

The existence of overmassive BHs (or undermassive galaxies) implies that heavy BH seeds form and grow prior to significant host galaxy assembly (e.g., Inayoshi et al. 2020; Volonteri et al. 2021). High-resolution simulations of galactic nuclei show that overmassive BHs can naturally form via super-Eddington accretion in high-redshift massive dark matter halos, where dense inflows sustain accretion far above the Eddington rate (Toyouchi et al. 2021; Sassano et al. 2023; Shi et al. 2023, 2024; Quadri et al. 2025). Photon trapping and inflow ram pressure suppress radiative

feedback and enable continuous BH growth (Inayoshi et al. 2016; Park et al. 2016; Sugimura et al. 2017; Takeo et al. 2020), although mechanical feedback may intermittently limit it (Regan et al. 2019; Massonneau et al. 2023; Kiyuna 2025; Lupi et al. 2024a). This process allows seed BHs to grow by  $\sim 1 - 2$  orders of magnitude before substantial stellar assembly, yielding  $M_{\text{BH}}/M_{\star} \simeq 0.1 - 1$  as predicted by radiation hydrodynamic simulations before the JWST launch (Inayoshi et al. 2022b).

In contrast, cosmological simulations generally predict delayed BH growth, as stellar feedback prevents nuclear gas retention until galaxies become sufficiently massive (e.g., Habouzit et al. 2017; Anglés-Alcázar et al. 2017; Dubois et al. 2021; Valentini et al. 2021; Habouzit et al. 2022; Zhu et al. 2022). Limited by sub-grid feedback models, these large-scale runs tend to produce “undermassive” BHs compared with the JWST-detected AGNs (see Habouzit 2025), highlighting the need for improved nuclear-scale feedback treatments. Recently, zoom-in cosmological simulations demonstrate that overmassive BHs can form via rapid gas accretion when the effective strengths of sub-grid feedback prescriptions are reduced (e.g., Wellons et al. 2023).

We note that the apparent high mass ratio may partially reflect selection biases toward strong emission-line sources and systematic uncertainties in BH mass estimates (Li et al. 2025b). Larger and less biased samples with improved BH mass measurements will be crucial to establish the intrinsic BH-galaxy connection in the early universe (e.g., Li et al. 2025a; Ding et al. 2025; Silverman et al. 2025). Nevertheless, the presence of extremely overmassive BHs with  $M_{\text{BH}}/M_{\star} > 0.1$  and potentially even higher in LRDs lacking host detections appears robust, as plausible combinations of systematic uncertainties (each at the  $\sim 0.3$  dex level) are insufficient to bring the ratios down to the local relation.

### 5.3. Other emission lines

#### 5.3.1. High-ionization lines

To study the origin of the UV emission observed in LRDs and to test their spectral models, it is useful to examine emission lines that require ionization potentials higher than the hydrogen ionization threshold  $E_{\text{H,ion}} = 13.6$  eV, such as He II  $\lambda 1640$ , He II  $\lambda 4686$ , C IV  $\lambda 1549$ , [N V]  $\lambda 1240$ , and [Ne V]  $\lambda 3426$  (e.g., Nakajima & Maiolino 2022; Übler et al. 2023; Lambrides et al. 2024; Scholtz et al. 2025). For reference, the ionization potentials for several key transitions are: He III (54.42 eV), C IV (47.89 eV), N IV (47.45 eV), N V (77.47 eV), Ne III (40.96 eV), Ne IV (63.42 eV), and Ne V (97.12 eV).

So far, high-ionization emission lines have been rarely detected in JWST spectra of LRDs (Labbé et al. 2024; Akins et al. 2025b; Wang et al. 2025b; Torralba et al. 2025a), either because the lines are intrinsically weak or the observations lack sufficient sensitivity, particularly in the faint UV regime. Marginal detections of He II  $\lambda 4686$  have been reported in some LRDs, but with very low line ratios of He II  $\lambda 4686/\text{H}\beta \sim 10^{-2}$ , less than 5% of the median value for local AGNs (Wang et al. 2025b). This observational result strongly constrains the ionizing spectral shape of LRDs. Their spectra must include hydrogen-ionizing photons, but lack the harder radiation required to doubly ionize helium. Such characteristics are consistent with a stellar-origin scenario for the UV emission. In particular, young, massive stars with very low, but nonzero metallicity ( $\simeq Z_{\odot}/50$ ) yield He II  $\lambda 4686/\text{H}\beta \simeq 8 \times 10^{-4}$  or a ratio between the hydrogen/ionized helium ionizing photon number fluxes,  $Q(\text{He}^+)/Q(\text{H}) \simeq 5 \times 10^{-4}$  (Schaerer 2002), consistent with the observed weakness of He II  $\lambda 4686$  emission.

On the other hand, a few LRDs do show high-ionization lines. For instance, Tang et al. (2025) reported narrow N V  $\lambda 1240$  emission in an LRD at  $z = 6.98$ , although neither C IV nor He II emission lines were observed. Because N V is unlikely produced by stellar processes, its detection likely requires nonstellar ionizing photons. One possible explanation is that the AGN radiation escapes through a funnel-like geometry aligned with the rotation axis. However, this “selective leakage” scenario faces a difficulty in explaining a lack of X-ray emission: if photons with  $E_{\text{ion}} > 70$  eV can escape, even higher-energy photons ( $\gtrsim$  keV X-rays) should also leak out since the photoionization cross section decreases with energy as  $\sigma_{\nu} \propto \nu^{-3}$ .

#### 5.3.2. Low-ionization lines

Another useful diagnostic comes from low-ionization metal lines with  $E_{\text{ion}} < 40$  eV. Classic narrow-line intensity ratio diagnostic diagrams, such as [O III]/ $\text{H}\beta$  vs. [N II]/ $\text{H}\alpha$  (Baldwin et al. 1981) or [O III]/ $\text{H}\beta$  vs. [Ne III]/[O II] (Backhaus et al. 2022) are commonly used to classify galaxies as dominated by emission from AGNs or star formation. However, JWST-identified AGNs (including both LRDs and more typical broad-line AGNs) tend to lie along the loci occupied by star-forming galaxies on these diagrams (Kocevski et al. 2023; Maiolino et al. 2024; Scholtz et al. 2025). This behavior is broadly consistent with photoionization models for low-metallicity AGNs, where reduced metal-line

cooling and altered relative element abundances (e.g.,  $N/O \propto Z$ ) shift line ratios toward the star-forming region (Hirschmann et al. 2019).

Nevertheless, some LRDs show intrinsically weak [O III] emission. For instance, Abell2744-QSO1 has a clear detection of [O III]  $\lambda 5007$  in its high-resolution spectrum (Ji et al. 2025a). However, the [O III]/ $H\beta$  ratio is extremely low, indicative of a very low gas-phase metallicity of  $\sim 0.01 Z_{\odot}$  (Maiolino et al. 2025b). The weakness of [O III] emission is attributed to spatially extended, less dense regions where collisional de-excitation would unlikely suppress the [O III] line, suggesting its metal-poor environment.

Complementing the oxygen lines, most LRDs also lack Fe II emission from both permitted and forbidden transitions (Trefoloni et al. 2025; but see also strong Fe II emission in some LRDs; Labbé et al. 2024 and Torralba et al. 2025b), even though Fe II emission is normally prominent in highly accreting, low-mass AGNs (Greene & Ho 2007; Shen & Ho 2014). The deficit of iron and  $\alpha$ -elements (e.g., C, O) thus reflects incomplete chemical enrichment in LRD nuclei, compared to quasar populations (e.g., Nagao et al. 2006; Onoue et al. 2020; Jiang et al. 2024). Furthermore, when AGNs are embedded in dense gas, resonance fluorescence of  $Ly\beta$  ( $n = 3 \rightarrow 1$ ) excites neutral oxygen and produces the O I ( $\lambda 1304$ ,  $\lambda 8446$ , and  $\lambda 11287$ ) emission lines (Kwan & Krolik 1981). These O I lines are observed in low-redshift AGNs as tracers of dense circumnuclear regions and correlate well with other low-ionization features such as Ca II and Fe II (e.g., Grandi 1980; Rodríguez-Ardila et al. 2002; Riffel et al. 2006; Matsuoka et al. 2007, 2008; Martínez-Aldama et al. 2015; Cracco et al. 2016). So far, two of the O I emission lines ( $\lambda 8446$  and  $\lambda 11287$ ) have been detected in some JWST-identified AGNs: GN-28074 at  $z = 2.26$  (Juodžbalis et al. 2024) and RUBIES-BLAGN-1 at  $z = 3.1$  (Wang et al. 2025a). Recently, Tripodi et al. (2025) reported an LRD at  $z = 5.3$  with the first high-redshift detection of the O I  $\lambda 1304$  bump (i.e., blend of O I  $\lambda 1304$  and Si II  $\lambda 1263$ ) together with O I  $\lambda 8446$  emission. Radiation-hydrodynamic simulations have suggested that detection of these O I lines with JWST/NIRSpec would provide a direct probe of dense, super-Eddington accretion flows around seed BHs (Inayoshi et al. 2022c).

#### 5.4. Environments

A useful approach to understanding the formation of LRDs and their connection to quasars in a cosmological context is to determine how these systems emerge within the evolving dark matter cosmic web. The clustering strength of a given population, or equivalently the size of the cosmic overdensities that they inhabit, provides a direct estimate of their typical host halo masses. Imaging analyses indicate that LRDs are not isolated but instead reside in moderately clustered environments, in contrast to UV-bright quasars whose host halos are expected to reach  $M_h \sim 10^{12} - 10^{13} M_{\odot}$  (e.g., Pizzati et al. 2025). Clustering analyses for LRDs with typical luminosities suggest substantially lower halo masses of  $M_h \simeq (0.6 - 3) \times 10^{11} M_{\odot}$  at  $z \simeq 4 - 6$ , consistent across multiple independent studies (Arita et al. 2025; Lin et al. 2025c). Notably, Schindler et al. (2025) recently reported the brightest LRD at  $z = 7.26$  ( $L_{bol} \simeq 4 \times 10^{45} \text{ erg s}^{-1}$ , 10 times higher if correcting dust reddening with  $A_V \sim 2.8 \text{ mag}$ ) embedded in a pronounced overdensity comparable to that of UV-luminous quasars at  $z \sim 6$ , implying a host halo mass of  $M_h \simeq 10^{12} M_{\odot}$ , the most strongly clustered LRD identified to date.

From the dark matter halo mass function (Sheth & Tormen 2002), the number density of such halos exceeds the observed LRD abundance ( $\phi_{LRD} \simeq 6 \times 10^{-5} \text{ Mpc}^{-3}$  at  $z \sim 4 - 8$ ; Kocevski et al. 2025; Kokorev et al. 2024a; Zhuang et al. 2025) by 2 orders of magnitude, implying a duty cycle of only  $\sim 1\%$ . This value is comparable to that of UV-luminous quasars (e.g., Davies et al. 2019; Eilers et al. 2021, 2024), suggesting that the LRD phase represents a short-lived stage of BH growth. Such brief active phases challenge current models of early BH formation, indicating that most BH mass assembly may occur in highly obscured or radiatively inefficient accretion episodes preceding the visible LRD stage.

#### 5.5. Alternatives

The lack of a definitive conclusion on the origin of early BHs leaves room for alternative, non-baryonic seeding scenarios. In the absence of clear signatures of host galaxies, gravothermal collapse in self-interacting dark matter (SIDM) halos provides a natural pathway for forming BHs in high-concentration halos with a characteristic mass scale determined by the SIDM cross section (Balberg & Shapiro 2002; Feng et al. 2021; Grant Roberts et al. 2025). This process occurs preferentially in the early universe and could account for the observed abundance of LRDs, apparently galaxy-less, early AGN hosting massive BHs (Jiang et al. 2025). Another possibility involves primordial black holes (PBHs), which can form from the collapse of early-universe density fluctuations or topological defects such as cosmic



strings (e.g., Carr 1975), or during phase transitions that temporarily render the universe pressureless (i.e., matter-dominated). For PBHs formed via critical collapse, the resulting mass spectrum depends sensitively on the primordial fluctuation power spectrum. A nearly monochromatic spectrum (e.g., Yokoyama 1998) produces PBHs with a narrow mass range, insufficient to explain both dark matter and supermassive BHs in galactic nuclei, whereas scale-invariant fluctuations yield a broader, power-law mass distribution (Harada et al. 2016). PBH-seeded models would result in extremely high  $M_{\text{BH}}/M_*$  values and describe low-metallicity environments of some LRDs (Dayal & Maiolino 2025; Maiolino et al. 2025b).

## 6. SUMMARY

LRDs are a newly discovered AGN population revealed by deep JWST observations. Their properties, such as compact morphology, red optical continua, and V-shaped SEDs, differ from the canonical AGN framework and have opened new perspectives on the earliest phases of BH growth. This review summarizes recent progress in understanding how accreting BHs can reproduce the characteristic LRD features, how their nuclear environments differ from those of normal AGNs, and how forthcoming observations can discriminate among competing scenarios.

JWST spectroscopic observations show that LRDs exhibit broad Balmer emission lines with FWHM  $\gtrsim 1,000 \text{ km s}^{-1}$ , consistent with the presence of accreting BHs with  $M_{\text{BH}} \simeq 10^6 - 10^7 M_\odot$ . In most cases, the optical luminosity of LRDs appears difficult to explain with stellar emission alone, although young stellar populations may still contribute to the UV continuum. The coexistence of broad emission with Balmer absorption and prominent Balmer breaks implies that the nuclear regions are heavily embedded in a dense gaseous medium with a high covering fraction. One promising interpretation is that LRDs host gas-enshrouded AGNs. In this scenario, a dense, potentially clumpy, gaseous envelope around the nucleus provides both gas attenuation and thermal self-emission with an effective temperature of  $T_{\text{eff}} \simeq 5000 \text{ K}$ . The resulting continuum emission accounts for the red optical and flat NIR spectra without requiring substantial dust reddening. Such a configuration also explains Balmer absorption and weak (short-term) variability, offering a possible connection to super-Eddington accretion episodes.

From both their spectral properties and their cosmic abundance evolution (rising from  $z > 10$  toward  $z \sim 6 - 7$  and declining to lower redshifts), LRDs can be interpreted as a transient phase in early BH growth, possibly corresponding to the first one or two accretion episodes of newborn BHs. As such, they may represent the long-sought missing link between BH seed formation and the emergence of luminous quasars.

Future observations will be crucial to test these scenarios. Improved monitoring campaigns to probe long-term variability, IFU observations to resolve nuclear gas kinematics and to map the spatial distribution of diagnostic emission lines, and clustering analysis of LRDs will provide key diagnostics of the central engine and its environment. In addition, polarization measurements, searches for post-LRD descendants, and studies of local analogs will offer complementary constraints on their physical nature. High-resolution spectroscopy and multi-wavelength campaigns with JWST, ALMA, and next-generation facilities will further constrain their energetics, metallicity, and feedback signatures. Finally, joint observations with future gravitational-wave experiments may probe the emergence of the earliest BHs, including channels involving non-baryonic origins.

## ACKNOWLEDGMENTS

We greatly thank Chang-Hao Chen, Subo Dong, Sihan Lu, Hao Wu, and Zijian Zhang for constructive discussions. K.I. and L.C.H. acknowledge support from the National Natural Science Foundation of China (12573015, 1251101148, 12233001, 12473037), and the China Manned Space Program (CMS-CSST-2025-A09).

## AUTHOR CONTRIBUTIONS

Both authors contributed equally.

## REFERENCES

- |  |  |
|--|--|
| <p>Aird, J., Coil, A. L., Georgakakis, A., et al. 2015, MNRAS, 451, 1892, doi: <a href="https://doi.org/10.1093/mnras/stv1062">10.1093/mnras/stv1062</a></p> | <p>Akins, H. B., Casey, C. M., Lambrides, E., et al. 2025a, ApJ, 991, 37, doi: <a href="https://doi.org/10.3847/1538-4357/ade984">10.3847/1538-4357/ade984</a></p> |
|--|--|



- Akins, H. B., Casey, C. M., Berg, D. A., et al. 2025b, *ApJL*, 980, L29, doi: [10.3847/2041-8213/adab76](https://doi.org/10.3847/2041-8213/adab76)
- Ananna, T. T., Bogdán, Á., Kovács, O. E., Natarajan, P., & Hickox, R. C. 2024, *ApJL*, 969, L18, doi: [10.3847/2041-8213/ad5669](https://doi.org/10.3847/2041-8213/ad5669)
- Ananna, T. T., Treister, E., Urry, C. M., et al. 2019, *ApJ*, 871, 240, doi: [10.3847/1538-4357/aafb77](https://doi.org/10.3847/1538-4357/aafb77)
- Anglés-Alcázar, D., Faucher-Giguère, C.-A., Quataert, E., et al. 2017, *MNRAS*, 472, L109, doi: [10.1093/mnras/slx161](https://doi.org/10.1093/mnras/slx161)
- Aoki, K., Iwata, I., Ohta, K., et al. 2006, *ApJ*, 651, 84, doi: [10.1086/507438](https://doi.org/10.1086/507438)
- Arita, J., Kashikawa, N., Onoue, M., et al. 2025, *MNRAS*, 536, 3677, doi: [10.1093/mnras/stae2765](https://doi.org/10.1093/mnras/stae2765)
- Backhaus, B. E., Trump, J. R., Cleri, N. J., et al. 2022, *ApJ*, 926, 161, doi: [10.3847/1538-4357/ac3919](https://doi.org/10.3847/1538-4357/ac3919)
- Baggen, J. F. W., van Dokkum, P., Brammer, G., et al. 2024, *ApJL*, 977, L13, doi: [10.3847/2041-8213/ad90b8](https://doi.org/10.3847/2041-8213/ad90b8)
- Balberg, S., & Shapiro, S. L. 2002, *PhRvL*, 88, 101301, doi: [10.1103/PhysRevLett.88.101301](https://doi.org/10.1103/PhysRevLett.88.101301)
- Baldwin, J. A. 1975, *ApJ*, 201, 26, doi: [10.1086/153855](https://doi.org/10.1086/153855)
- Baldwin, J. A., Ferland, G. J., Martin, P. G., et al. 1991, *ApJ*, 374, 580, doi: [10.1086/170146](https://doi.org/10.1086/170146)
- Baldwin, J. A., Phillips, M. M., & Terlevich, R. 1981, *PASP*, 93, 5, doi: [10.1086/130766](https://doi.org/10.1086/130766)
- Barro, G., Pérez-González, P. G., Kocevski, D. D., et al. 2024, *ApJ*, 963, 128, doi: [10.3847/1538-4357/ad167e](https://doi.org/10.3847/1538-4357/ad167e)
- Barvainis, R. 1987, *ApJ*, 320, 537, doi: [10.1086/165571](https://doi.org/10.1086/165571)
- Begelman, M. C., & Dexter, J. 2025, arXiv e-prints, arXiv:2507.09085, doi: [10.48550/arXiv.2507.09085](https://doi.org/10.48550/arXiv.2507.09085)
- Begelman, M. C., Rossi, E. M., & Armitage, P. J. 2008, *MNRAS*, 387, 1649, doi: [10.1111/j.1365-2966.2008.13344.x](https://doi.org/10.1111/j.1365-2966.2008.13344.x)
- Begelman, M. C., Volonteri, M., & Rees, M. J. 2006, *MNRAS*, 370, 289, doi: [10.1111/j.1365-2966.2006.10467.x](https://doi.org/10.1111/j.1365-2966.2006.10467.x)
- Bell, E. F., & de Jong, R. S. 2001, *ApJ*, 550, 212, doi: [10.1086/319728](https://doi.org/10.1086/319728)
- Bentz, M. C., Peterson, B. M., Netzer, H., Pogge, R. W., & Vestergaard, M. 2009, *ApJ*, 697, 160, doi: [10.1088/0004-637X/697/1/160](https://doi.org/10.1088/0004-637X/697/1/160)
- Billand, J.-B., Elbaz, D., Gentile, F., et al. 2025, arXiv e-prints, arXiv:2507.04011, doi: [10.48550/arXiv.2507.04011](https://doi.org/10.48550/arXiv.2507.04011)
- Bouwens, R. J., Oesch, P. A., Stefanon, M., et al. 2021, *AJ*, 162, 47, doi: [10.3847/1538-3881/abf83e](https://doi.org/10.3847/1538-3881/abf83e)
- Boylan-Kolchin, M. 2023, *Nature Astronomy*, doi: [10.1038/s41550-023-01937-7](https://doi.org/10.1038/s41550-023-01937-7)
- Brandt, W. N., Laor, A., & Wills, B. J. 2000, *ApJ*, 528, 637, doi: [10.1086/308207](https://doi.org/10.1086/308207)
- Burke, C. J., Shen, Y., Blaes, O., et al. 2021, *Science*, 373, 789, doi: [10.1126/science.abg9933](https://doi.org/10.1126/science.abg9933)
- Calzetti, D., Kinney, A. L., & Storchi-Bergmann, T. 1994, *ApJ*, 429, 582, doi: [10.1086/174346](https://doi.org/10.1086/174346)
- Carr, B. J. 1975, *ApJ*, 201, 1, doi: [10.1086/153853](https://doi.org/10.1086/153853)
- Casey, C. M., Akins, H. B., Kokorev, V., et al. 2024, *ApJL*, 975, L4, doi: [10.3847/2041-8213/ad7ba7](https://doi.org/10.3847/2041-8213/ad7ba7)
- Casey, C. M., Akins, H. B., Finkelstein, S. L., et al. 2025, *ApJL*, 990, L61, doi: [10.3847/2041-8213/adfa91](https://doi.org/10.3847/2041-8213/adfa91)
- Chang, S.-J., Gronke, M., Matthee, J., & Mason, C. 2025, arXiv e-prints, arXiv:2508.08768, doi: [10.48550/arXiv.2508.08768](https://doi.org/10.48550/arXiv.2508.08768)
- Chen, C.-H., Ho, L. C., Li, R., & Inayoshi, K. 2025a, *ApJL*, 989, L12, doi: [10.3847/2041-8213/adee0a](https://doi.org/10.3847/2041-8213/adee0a)
- Chen, C.-H., Ho, L. C., Li, R., & Zhuang, M.-Y. 2025b, *ApJ*, 983, 60, doi: [10.3847/1538-4357/ada93a](https://doi.org/10.3847/1538-4357/ada93a)
- Chen, K., Li, Z., Inayoshi, K., & Ho, L. C. 2025c, arXiv e-prints, arXiv:2505.22600, doi: [10.48550/arXiv.2505.22600](https://doi.org/10.48550/arXiv.2505.22600)
- Comastri, A., Lanzuisi, G., Vito, F., et al. 2025, arXiv e-prints, arXiv:2510.00112, doi: [10.48550/arXiv.2510.00112](https://doi.org/10.48550/arXiv.2510.00112)
- Coughlin, E. R., & Begelman, M. C. 2024, *ApJ*, 970, 158, doi: [10.3847/1538-4357/ad5723](https://doi.org/10.3847/1538-4357/ad5723)
- Cracco, V., Ciroi, S., Berton, M., et al. 2016, *MNRAS*, 462, 1256, doi: [10.1093/mnras/stw1689](https://doi.org/10.1093/mnras/stw1689)
- Davies, F. B., Hennawi, J. F., & Eilers, A.-C. 2019, *ApJL*, 884, L19, doi: [10.3847/2041-8213/ab42e3](https://doi.org/10.3847/2041-8213/ab42e3)
- Dayal, P., & Maiolino, R. 2025, arXiv e-prints, arXiv:2506.08116, doi: [10.48550/arXiv.2506.08116](https://doi.org/10.48550/arXiv.2506.08116)
- de Graaff, A., Rix, H.-W., Naidu, R. P., et al. 2025, *A&A*, 701, A168, doi: [10.1051/0004-6361/202554681](https://doi.org/10.1051/0004-6361/202554681)
- Dekel, A., Sarkar, K. C., Birnboim, Y., Mandelker, N., & Li, Z. 2023, *MNRAS*, 523, 3201, doi: [10.1093/mnras/stad1557](https://doi.org/10.1093/mnras/stad1557)
- Dekel, A., Zolotov, A., Tweed, D., et al. 2013, *MNRAS*, 435, 999, doi: [10.1093/mnras/stt1338](https://doi.org/10.1093/mnras/stt1338)
- Delvecchio, I., Gruppioni, C., Pozzi, F., et al. 2014, *MNRAS*, 439, 2736, doi: [10.1093/mnras/stu130](https://doi.org/10.1093/mnras/stu130)
- Delvecchio, I., Daddi, E., Magnelli, B., et al. 2025, arXiv e-prints, arXiv:2509.07100, doi: [10.48550/arXiv.2509.07100](https://doi.org/10.48550/arXiv.2509.07100)
- D'Eugenio, F., Maiolino, R., Perna, M., et al. 2025, arXiv e-prints, arXiv:2503.11752, doi: [10.48550/arXiv.2503.11752](https://doi.org/10.48550/arXiv.2503.11752)
- Ding, X., Onoue, M., Silverman, J. D., et al. 2023, *Nature*, 621, 51, doi: [10.1038/s41586-023-06345-5](https://doi.org/10.1038/s41586-023-06345-5)
- . 2025, *ApJ*, 993, 91, doi: [10.3847/1538-4357/ae045b](https://doi.org/10.3847/1538-4357/ae045b)
- Dong, R., Greene, J. E., & Ho, L. C. 2012, *ApJ*, 761, 73, doi: [10.1088/0004-637X/761/1/73](https://doi.org/10.1088/0004-637X/761/1/73)

- Dong, X., Wang, T., Wang, J., et al. 2008, *MNRAS*, 383, 581, doi: [10.1111/j.1365-2966.2007.12560.x](https://doi.org/10.1111/j.1365-2966.2007.12560.x)
- Du, P., Hu, C., Lu, K.-X., et al. 2014, *ApJ*, 782, 45, doi: [10.1088/0004-637X/782/1/45](https://doi.org/10.1088/0004-637X/782/1/45)
- Du, P., Lu, K.-X., Zhang, Z.-X., et al. 2016, *ApJ*, 825, 126, doi: [10.3847/0004-637X/825/2/126](https://doi.org/10.3847/0004-637X/825/2/126)
- Dubois, Y., Beckmann, R., Bournaud, F., et al. 2021, *A&A*, 651, A109, doi: [10.1051/0004-6361/202039429](https://doi.org/10.1051/0004-6361/202039429)
- Eilers, A.-C., Hennawi, J. F., Davies, F. B., & Simcoe, R. A. 2021, *ApJ*, 917, 38, doi: [10.3847/1538-4357/ac0a76](https://doi.org/10.3847/1538-4357/ac0a76)
- Eilers, A.-C., Mackenzie, R., Pizzati, E., et al. 2024, *ApJ*, 974, 275, doi: [10.3847/1538-4357/ad778b](https://doi.org/10.3847/1538-4357/ad778b)
- Euclid Collaboration, Bisigello, L., Rodighiero, G., et al. 2025, arXiv e-prints, arXiv:2503.15323, doi: [10.48550/arXiv.2503.15323](https://doi.org/10.48550/arXiv.2503.15323)
- Fakhouri, O., Ma, C.-P., & Boylan-Kolchin, M. 2010, *MNRAS*, 406, 2267, doi: [10.1111/j.1365-2966.2010.16859.x](https://doi.org/10.1111/j.1365-2966.2010.16859.x)
- Feng, W.-X., Yu, H.-B., & Zhong, Y.-M. 2021, *ApJL*, 914, L26, doi: [10.3847/2041-8213/ac04b0](https://doi.org/10.3847/2041-8213/ac04b0)
- Finkelstein, S. L., Ryan, Russell E., J., Papovich, C., et al. 2015, *ApJ*, 810, 71, doi: [10.1088/0004-637X/810/1/71](https://doi.org/10.1088/0004-637X/810/1/71)
- Fowler, W. A. 1964, *Reviews of Modern Physics*, 36, 545, doi: [10.1103/RevModPhys.36.545](https://doi.org/10.1103/RevModPhys.36.545)
- Fujimoto, S., Kohno, K., Ouchi, M., et al. 2024, *ApJS*, 275, 36, doi: [10.3847/1538-4365/ad5ae2](https://doi.org/10.3847/1538-4365/ad5ae2)
- Furtak, L. J., Labbé, I., Zitrin, A., et al. 2024, *Nature*, 628, 57, doi: [10.1038/s41586-024-07184-8](https://doi.org/10.1038/s41586-024-07184-8)
- Furtak, L. J., Secunda, A. R., Greene, J. E., et al. 2025, *A&A*, 698, A227, doi: [10.1051/0004-6361/202554110](https://doi.org/10.1051/0004-6361/202554110)
- Gaskell, C. M., Goosmann, R. W., Antonucci, R. R. J., & Whysong, D. H. 2004, *ApJ*, 616, 147, doi: [10.1086/423885](https://doi.org/10.1086/423885)
- Gludemans, A. J., Duncan, K. J., Eilers, A.-C., et al. 2025, *ApJ*, 986, 130, doi: [10.3847/1538-4357/adddb9](https://doi.org/10.3847/1538-4357/adddb9)
- Grandi, S. A. 1980, *ApJ*, 238, 10, doi: [10.1086/157952](https://doi.org/10.1086/157952)
- Grant Roberts, M., Braff, L., Garg, A., et al. 2025, *JCAP*, 2025, 060, doi: [10.1088/1475-7516/2025/01/060](https://doi.org/10.1088/1475-7516/2025/01/060)
- Greene, J. E., & Ho, L. C. 2005, *ApJ*, 630, 122, doi: [10.1086/431897](https://doi.org/10.1086/431897)
- . 2007, *ApJ*, 670, 92, doi: [10.1086/522082](https://doi.org/10.1086/522082)
- Greene, J. E., Strader, J., & Ho, L. C. 2020, *ARA&A*, 58, 257, doi: [10.1146/annurev-astro-032620-021835](https://doi.org/10.1146/annurev-astro-032620-021835)
- Greene, J. E., Labbe, I., Goulding, A. D., et al. 2024, *ApJ*, 964, 39, doi: [10.3847/1538-4357/ad1e5f](https://doi.org/10.3847/1538-4357/ad1e5f)
- Greene, J. E., Setton, D. J., Furtak, L. J., et al. 2025, arXiv e-prints, arXiv:2509.05434, doi: [10.48550/arXiv.2509.05434](https://doi.org/10.48550/arXiv.2509.05434)
- Habouzit, M. 2025, *MNRAS*, 537, 2323, doi: [10.1093/mnras/staf167](https://doi.org/10.1093/mnras/staf167)
- Habouzit, M., Volonteri, M., & Dubois, Y. 2017, *MNRAS*, 468, 3935, doi: [10.1093/mnras/stx666](https://doi.org/10.1093/mnras/stx666)
- Habouzit, M., Onoue, M., Bañados, E., et al. 2022, *MNRAS*, doi: [10.1093/mnras/stac225](https://doi.org/10.1093/mnras/stac225)
- Hainline, K. N., Maiolino, R., Juodžbalis, I., et al. 2025, *ApJ*, 979, 138, doi: [10.3847/1538-4357/ad9920](https://doi.org/10.3847/1538-4357/ad9920)
- Harada, T., Yoo, C.-m., Kohri, K., Nakao, K.-i., & Jhingan, S. 2016, *ApJ*, 833, 61, doi: [10.3847/1538-4357/833/1/61](https://doi.org/10.3847/1538-4357/833/1/61)
- Harikane, Y., Nakajima, K., Ouchi, M., et al. 2024, *ApJ*, 960, 56, doi: [10.3847/1538-4357/ad0b7e](https://doi.org/10.3847/1538-4357/ad0b7e)
- Harikane, Y., Ono, Y., Ouchi, M., et al. 2022, *ApJS*, 259, 20, doi: [10.3847/1538-4365/ac3dfc](https://doi.org/10.3847/1538-4365/ac3dfc)
- Harikane, Y., Zhang, Y., Nakajima, K., et al. 2023, *ApJ*, 959, 39, doi: [10.3847/1538-4357/ad029e](https://doi.org/10.3847/1538-4357/ad029e)
- Hayashi, C. 1961, *PASJ*, 13, 450
- Hayashi, C., Hōshi, R., & Sugimoto, D. 1962, *Progress of Theoretical Physics Supplement*, 22, 1, doi: [10.1143/PTPS.22.1](https://doi.org/10.1143/PTPS.22.1)
- Hayes, M. J., Tan, J. C., Ellis, R. S., et al. 2024, *ApJL*, 971, L16, doi: [10.3847/2041-8213/ad63a7](https://doi.org/10.3847/2041-8213/ad63a7)
- Hickox, R. C., & Alexander, D. M. 2018, *ARA&A*, 56, 625, doi: [10.1146/annurev-astro-081817-051803](https://doi.org/10.1146/annurev-astro-081817-051803)
- Hirschmann, M., Charlot, S., Feltre, A., et al. 2019, *MNRAS*, 487, 333, doi: [10.1093/mnras/stz1256](https://doi.org/10.1093/mnras/stz1256)
- Ho, L. C. 1999, *ApJ*, 510, 631, doi: [10.1086/306597](https://doi.org/10.1086/306597)
- . 2008, *ARA&A*, 46, 475, doi: [10.1146/annurev.astro.45.051806.110546](https://doi.org/10.1146/annurev.astro.45.051806.110546)
- Ho, L. C., Filippenko, A. V., & Sargent, W. L. 1995, *ApJS*, 98, 477, doi: [10.1086/192170](https://doi.org/10.1086/192170)
- Ho, L. C., & Peng, C. Y. 2001, *ApJ*, 555, 650, doi: [10.1086/321524](https://doi.org/10.1086/321524)
- Hönig, S. F., & Kishimoto, M. 2010, *A&A*, 523, A27, doi: [10.1051/0004-6361/200912676](https://doi.org/10.1051/0004-6361/200912676)
- Hopkins, P. F., Murray, N., Quataert, E., & Thompson, T. A. 2010, *MNRAS*, 401, L19, doi: [10.1111/j.1745-3933.2009.00777.x](https://doi.org/10.1111/j.1745-3933.2009.00777.x)
- Hopkins, P. F., & Quataert, E. 2010, *MNRAS*, 407, 1529, doi: [10.1111/j.1365-2966.2010.17064.x](https://doi.org/10.1111/j.1365-2966.2010.17064.x)
- Hosokawa, T., Yorke, H. W., Inayoshi, K., Omukai, K., & Yoshida, N. 2013, *ApJ*, 778, 178, doi: [10.1088/0004-637X/778/2/178](https://doi.org/10.1088/0004-637X/778/2/178)
- Hoyle, F., Fowler, W. A., Burbidge, G. R., & Burbidge, E. M. 1964, *ApJ*, 139, 909, doi: [10.1086/147825](https://doi.org/10.1086/147825)
- Hu, H., Inayoshi, K., Haiman, Z., Quataert, E., & Kuiper, R. 2022, *ApJ*, 934, 132, doi: [10.3847/1538-4357/ac75d8](https://doi.org/10.3847/1538-4357/ac75d8)
- Hviding, R. E., de Graaff, A., Miller, T. B., et al. 2025, *A&A*, 702, A57, doi: [10.1051/0004-6361/202555816](https://doi.org/10.1051/0004-6361/202555816)
- Ichikawa, K., Ricci, C., Ueda, Y., et al. 2019, *ApJ*, 870, 31, doi: [10.3847/1538-4357/aaef8f](https://doi.org/10.3847/1538-4357/aaef8f)

- Inayoshi, K. 2025, *ApJL*, 988, L22, doi: [10.3847/2041-8213/adea66](https://doi.org/10.3847/2041-8213/adea66)
- Inayoshi, K., Haiman, Z., & Ostriker, J. P. 2016, *MNRAS*, 459, 3738, doi: [10.1093/mnras/stw836](https://doi.org/10.1093/mnras/stw836)
- Inayoshi, K., Harikane, Y., Inoue, A. K., Li, W., & Ho, L. C. 2022a, *ApJL*, 938, L10, doi: [10.3847/2041-8213/ac9310](https://doi.org/10.3847/2041-8213/ac9310)
- Inayoshi, K., & Ichikawa, K. 2024, *ApJL*, 973, L49, doi: [10.3847/2041-8213/ad74e2](https://doi.org/10.3847/2041-8213/ad74e2)
- Inayoshi, K., Kimura, S. S., & Noda, H. 2025a, *PASJ*, 77, 811, doi: [10.1093/pasj/psaf050](https://doi.org/10.1093/pasj/psaf050)
- Inayoshi, K., & Maiolino, R. 2025, *ApJL*, 980, L27, doi: [10.3847/2041-8213/adaebd](https://doi.org/10.3847/2041-8213/adaebd)
- Inayoshi, K., Murase, K., & Kashiyama, K. 2025b, *arXiv e-prints*, arXiv:2509.19422, doi: [10.48550/arXiv.2509.19422](https://doi.org/10.48550/arXiv.2509.19422)
- Inayoshi, K., Nakatani, R., Toyouchi, D., et al. 2022b, *ApJ*, 927, 237, doi: [10.3847/1538-4357/ac4751](https://doi.org/10.3847/1538-4357/ac4751)
- Inayoshi, K., Onoue, M., Sugahara, Y., Inoue, A. K., & Ho, L. C. 2022c, *ApJL*, 931, L25, doi: [10.3847/2041-8213/ac6f01](https://doi.org/10.3847/2041-8213/ac6f01)
- Inayoshi, K., Shangguan, J., Chen, X., Ho, L. C., & Haiman, Z. 2025c, *arXiv e-prints*, arXiv:2505.05322, doi: [10.48550/arXiv.2505.05322](https://doi.org/10.48550/arXiv.2505.05322)
- Inayoshi, K., Visbal, E., & Haiman, Z. 2020, *ARA&A*, 58, 27, doi: [10.1146/annurev-astro-120419-014455](https://doi.org/10.1146/annurev-astro-120419-014455)
- Into, T., & Portinari, L. 2013, *MNRAS*, 430, 2715, doi: [10.1093/mnras/stt071](https://doi.org/10.1093/mnras/stt071)
- Ji, X., Maiolino, R., Übler, H., et al. 2025a, *arXiv e-prints*, arXiv:2501.13082, doi: [10.48550/arXiv.2501.13082](https://doi.org/10.48550/arXiv.2501.13082)
- Ji, X., D'Eugenio, F., Juodžbalis, I., et al. 2025b, *arXiv e-prints*, arXiv:2507.23774, doi: [10.48550/arXiv.2507.23774](https://doi.org/10.48550/arXiv.2507.23774)
- Jiang, D., Onoue, M., Jiang, L., et al. 2024, *ApJ*, 975, 214, doi: [10.3847/1538-4357/ad7d09](https://doi.org/10.3847/1538-4357/ad7d09)
- Jiang, F., Jia, Z., Zheng, H., et al. 2025, *arXiv e-prints*, arXiv:2503.23710, doi: [10.48550/arXiv.2503.23710](https://doi.org/10.48550/arXiv.2503.23710)
- Jones, B. L., Kocevski, D. D., Pacucci, F., et al. 2025, *arXiv e-prints*, arXiv:2510.07376, doi: [10.48550/arXiv.2510.07376](https://doi.org/10.48550/arXiv.2510.07376)
- Juodžbalis, I., Ji, X., Maiolino, R., et al. 2024, *MNRAS*, 535, 853, doi: [10.1093/mnras/stae2367](https://doi.org/10.1093/mnras/stae2367)
- Juodžbalis, I., Maiolino, R., Baker, W. M., et al. 2025a, *arXiv e-prints*, arXiv:2504.03551, doi: [10.48550/arXiv.2504.03551](https://doi.org/10.48550/arXiv.2504.03551)
- Juodžbalis, I., Marconcini, C., D'Eugenio, F., et al. 2025b, *arXiv e-prints*, arXiv:2508.21748, doi: [10.48550/arXiv.2508.21748](https://doi.org/10.48550/arXiv.2508.21748)
- Kaspi, S., Smith, P. S., Netzer, H., et al. 2000, *ApJ*, 533, 631, doi: [10.1086/308704](https://doi.org/10.1086/308704)
- Kido, D., Ioka, K., Hotokezaka, K., Inayoshi, K., & Irwin, C. M. 2025, *MNRAS*, 544, 3407, doi: [10.1093/mnras/staf1898](https://doi.org/10.1093/mnras/staf1898)
- Killi, M., Watson, D., Brammer, G., et al. 2024, *A&A*, 691, A52, doi: [10.1051/0004-6361/202348857](https://doi.org/10.1051/0004-6361/202348857)
- Kiyuna, M. 2025, *arXiv e-prints*, arXiv:2506.15781, doi: [10.48550/arXiv.2506.15781](https://doi.org/10.48550/arXiv.2506.15781)
- Kocevski, D. D., Onoue, M., Inayoshi, K., et al. 2023, *ApJL*, 954, L4, doi: [10.3847/2041-8213/ace5a0](https://doi.org/10.3847/2041-8213/ace5a0)
- Kocevski, D. D., Finkelstein, S. L., Barro, G., et al. 2025, *ApJ*, 986, 126, doi: [10.3847/1538-4357/adbc7d](https://doi.org/10.3847/1538-4357/adbc7d)
- Kokorev, V., Caputi, K. I., Greene, J. E., et al. 2024a, *ApJ*, 968, 38, doi: [10.3847/1538-4357/ad4265](https://doi.org/10.3847/1538-4357/ad4265)
- Kokorev, V., Chisholm, J., Endsley, R., et al. 2024b, *ApJ*, 975, 178, doi: [10.3847/1538-4357/ad7d03](https://doi.org/10.3847/1538-4357/ad7d03)
- Kokubo, M., & Harikane, Y. 2024, *arXiv e-prints*, arXiv:2407.04777, doi: [10.48550/arXiv.2407.04777](https://doi.org/10.48550/arXiv.2407.04777)
- Kormendy, J., & Ho, L. C. 2013, *ARA&A*, 51, 511, doi: [10.1146/annurev-astro-082708-101811](https://doi.org/10.1146/annurev-astro-082708-101811)
- Krolik, J. H., & McKee, C. F. 1978, *ApJS*, 37, 459, doi: [10.1086/190538](https://doi.org/10.1086/190538)
- Kwan, J., & Krolik, J. H. 1981, *ApJ*, 250, 478, doi: [10.1086/159395](https://doi.org/10.1086/159395)
- Labbé, I., Greene, J. E., Matthee, J., et al. 2024, *arXiv e-prints*, arXiv:2412.04557, doi: [10.48550/arXiv.2412.04557](https://doi.org/10.48550/arXiv.2412.04557)
- Labbé, I., Greene, J. E., Bezanson, R., et al. 2025, *ApJ*, 978, 92, doi: [10.3847/1538-4357/ad3551](https://doi.org/10.3847/1538-4357/ad3551)
- Lambrides, E., Garofali, K., Larson, R., et al. 2024, *arXiv e-prints*, arXiv:2409.13047, doi: [10.48550/arXiv.2409.13047](https://doi.org/10.48550/arXiv.2409.13047)
- Laor, A. 2006, *ApJ*, 643, 112, doi: [10.1086/502798](https://doi.org/10.1086/502798)
- Laurenti, M., Piconcelli, E., Zappacosta, L., et al. 2022, *A&A*, 657, A57, doi: [10.1051/0004-6361/202141829](https://doi.org/10.1051/0004-6361/202141829)
- Li, J., Shen, Y., & Zhuang, M.-Y. 2025a, *arXiv e-prints*, arXiv:2502.05048, doi: [10.48550/arXiv.2502.05048](https://doi.org/10.48550/arXiv.2502.05048)
- Li, J., Silverman, J. D., Shen, Y., et al. 2025b, *ApJ*, 981, 19, doi: [10.3847/1538-4357/ada603](https://doi.org/10.3847/1538-4357/ada603)
- Li, R., Ho, L. C., & Chen, C.-H. 2025c, *arXiv e-prints*, arXiv:2505.12867, doi: [10.48550/arXiv.2505.12867](https://doi.org/10.48550/arXiv.2505.12867)
- Li, Z., Inayoshi, K., Chen, K., Ichikawa, K., & Ho, L. C. 2025d, *ApJ*, 980, 36, doi: [10.3847/1538-4357/ada5fb](https://doi.org/10.3847/1538-4357/ada5fb)
- Lin, R., Zheng, Z.-Y., Jiang, C., et al. 2025a, *ApJL*, 980, L34, doi: [10.3847/2041-8213/adaaf1](https://doi.org/10.3847/2041-8213/adaaf1)
- Lin, X., Wang, F., Fan, X., et al. 2024, *ApJ*, 974, 147, doi: [10.3847/1538-4357/ad6565](https://doi.org/10.3847/1538-4357/ad6565)
- Lin, X., Fan, X., Cai, Z., et al. 2025b, *arXiv e-prints*, arXiv:2507.10659, <https://arxiv.org/abs/2507.10659>
- Lin, X., Fan, X., Sun, F., et al. 2025c, *arXiv e-prints*, arXiv:2505.02896, doi: [10.48550/arXiv.2505.02896](https://doi.org/10.48550/arXiv.2505.02896)

- Liu, H., Jiang, Y.-F., Quataert, E., Greene, J. E., & Ma, Y. 2025, *ApJ*, 994, 113, doi: [10.3847/1538-4357/ae0c19](https://doi.org/10.3847/1538-4357/ae0c19)
- Liu, H., Luo, B., Brandt, W. N., et al. 2021, *ApJ*, 910, 103, doi: [10.3847/1538-4357/abe37f](https://doi.org/10.3847/1538-4357/abe37f)
- Lupi, A., Quadri, G., Volonteri, M., Colpi, M., & Regan, J. A. 2024a, *A&A*, 686, A256, doi: [10.1051/0004-6361/202348788](https://doi.org/10.1051/0004-6361/202348788)
- Lupi, A., Trinca, A., Volonteri, M., Dotti, M., & Mazzucchelli, C. 2024b, *A&A*, 689, A128, doi: [10.1051/0004-6361/202451249](https://doi.org/10.1051/0004-6361/202451249)
- Lusso, E., Worsack, G., Hennawi, J. F., et al. 2015, *MNRAS*, 449, 4204, doi: [10.1093/mnras/stv516](https://doi.org/10.1093/mnras/stv516)
- Lusso, E., Risaliti, G., Nardini, E., et al. 2020, *A&A*, 642, A150, doi: [10.1051/0004-6361/202038899](https://doi.org/10.1051/0004-6361/202038899)
- Lynden-Bell, D. 1969, *Nature*, 223, 690, doi: [10.1038/223690a0](https://doi.org/10.1038/223690a0)
- Lynden-Bell, D., & Rees, M. J. 1971, *MNRAS*, 152, 461, doi: [10.1093/mnras/152.4.461](https://doi.org/10.1093/mnras/152.4.461)
- Lyu, J., Alberts, S., Rieke, G. H., et al. 2024, *ApJ*, 966, 229, doi: [10.3847/1538-4357/ad3643](https://doi.org/10.3847/1538-4357/ad3643)
- Ma, Y., Greene, J. E., Setton, D. J., et al. 2025a, *ApJ*, 981, 191, doi: [10.3847/1538-4357/ada613](https://doi.org/10.3847/1538-4357/ada613)
- . 2025b, arXiv e-prints, arXiv:2504.08032, doi: [10.48550/arXiv.2504.08032](https://doi.org/10.48550/arXiv.2504.08032)
- Madau, P., & Dickinson, M. 2014, *ARA&A*, 52, 415, doi: [10.1146/annurev-astro-081811-125615](https://doi.org/10.1146/annurev-astro-081811-125615)
- Madau, P., & Haardt, F. 2024, *ApJL*, 976, L24, doi: [10.3847/2041-8213/ad90e1](https://doi.org/10.3847/2041-8213/ad90e1)
- Maiolino, R., Scholtz, J., Curtis-Lake, E., et al. 2024, *A&A*, 691, A145, doi: [10.1051/0004-6361/202347640](https://doi.org/10.1051/0004-6361/202347640)
- Maiolino, R., Risaliti, G., Signorini, M., et al. 2025a, *MNRAS*, 538, 1921, doi: [10.1093/mnras/staf359](https://doi.org/10.1093/mnras/staf359)
- Maiolino, R., Uebler, H., D'Eugenio, F., et al. 2025b, arXiv e-prints, arXiv:2505.22567, doi: [10.48550/arXiv.2505.22567](https://doi.org/10.48550/arXiv.2505.22567)
- Markov, V., Gallerani, S., Ferrara, A., et al. 2025, *Nature Astronomy*, 9, 458, doi: [10.1038/s41550-024-02426-1](https://doi.org/10.1038/s41550-024-02426-1)
- Martínez-Aldama, M. L., Dultzin, D., Marziani, P., et al. 2015, *ApJS*, 217, 3, doi: [10.1088/0067-0049/217/1/3](https://doi.org/10.1088/0067-0049/217/1/3)
- Massonneau, W., Volonteri, M., Dubois, Y., & Beckmann, R. S. 2023, *A&A*, 670, A180, doi: [10.1051/0004-6361/202243170](https://doi.org/10.1051/0004-6361/202243170)
- Mathis, J. S. 1970, *ApJ*, 159, 263, doi: [10.1086/150308](https://doi.org/10.1086/150308)
- . 1983, *ApJ*, 267, 119, doi: [10.1086/160849](https://doi.org/10.1086/160849)
- Matsuoka, Y., Kawara, K., & Oyabu, S. 2008, *ApJ*, 673, 62, doi: [10.1086/524193](https://doi.org/10.1086/524193)
- Matsuoka, Y., Oyabu, S., Tsuzuki, Y., & Kawara, K. 2007, *ApJ*, 663, 781, doi: [10.1086/518399](https://doi.org/10.1086/518399)
- Matthee, J., Naidu, R. P., Brammer, G., et al. 2024, *ApJ*, 963, 129, doi: [10.3847/1538-4357/ad2345](https://doi.org/10.3847/1538-4357/ad2345)
- Mayer, L., Capelo, P. R., Zwick, L., & Di Matteo, T. 2024, *ApJ*, 961, 76, doi: [10.3847/1538-4357/ad11cf](https://doi.org/10.3847/1538-4357/ad11cf)
- Mazzolari, G., Gilli, R., Maiolino, R., et al. 2024, arXiv e-prints, arXiv:2412.04224, doi: [10.48550/arXiv.2412.04224](https://doi.org/10.48550/arXiv.2412.04224)
- Mérida, R. M., Gaspar, G., Asada, Y., et al. 2025, arXiv e-prints, arXiv:2510.06408, doi: [10.48550/arXiv.2510.06408](https://doi.org/10.48550/arXiv.2510.06408)
- Merloni, A., Heinz, S., & di Matteo, T. 2003, *MNRAS*, 345, 1057, doi: [10.1046/j.1365-2966.2003.07017.x](https://doi.org/10.1046/j.1365-2966.2003.07017.x)
- Nagao, T., Marconi, A., & Maiolino, R. 2006, *A&A*, 447, 157, doi: [10.1051/0004-6361:20054024](https://doi.org/10.1051/0004-6361:20054024)
- Naidu, R. P., Matthee, J., Katz, H., et al. 2025, arXiv e-prints, arXiv:2503.16596, doi: [10.48550/arXiv.2503.16596](https://doi.org/10.48550/arXiv.2503.16596)
- Nakajima, K., & Maiolino, R. 2022, *MNRAS*, 513, 5134, doi: [10.1093/mnras/stac1242](https://doi.org/10.1093/mnras/stac1242)
- Nandal, D., & Loeb, A. 2025, arXiv e-prints, arXiv:2507.12618, doi: [10.48550/arXiv.2507.12618](https://doi.org/10.48550/arXiv.2507.12618)
- Nandra, K., Laird, E. S., Aird, J. A., et al. 2015, *ApJS*, 220, 10, doi: [10.1088/0067-0049/220/1/10](https://doi.org/10.1088/0067-0049/220/1/10)
- Nikopoulos, G. P., Watson, D., Sneppen, A., et al. 2025, arXiv e-prints, arXiv:2510.06362, doi: [10.48550/arXiv.2510.06362](https://doi.org/10.48550/arXiv.2510.06362)
- Novikov, I. D., & Thorne, K. S. 1973, in *Black Holes (Les Astres Occlus)*, 343–450
- Onoue, M., Bañados, E., Mazzucchelli, C., et al. 2020, *ApJ*, 898, 105, doi: [10.3847/1538-4357/aba193](https://doi.org/10.3847/1538-4357/aba193)
- Osterbrock, D. E. 1974, *Astrophysics of gaseous nebulae*, 1st ed., Freeman and Company, San Francisco, CA
- Osterbrock, D. E., & Ferland, G. J. 2006, *Astrophysics of gaseous nebulae and active galactic nuclei*, 2nd edn. University Science Books, Sausalito, CA
- Pacucci, F., Hernquist, L., & Fujii, M. 2025, arXiv e-prints, arXiv:2509.02664, doi: [10.48550/arXiv.2509.02664](https://doi.org/10.48550/arXiv.2509.02664)
- Pacucci, F., & Narayan, R. 2024, *ApJ*, 976, 96, doi: [10.3847/1538-4357/ad84f7](https://doi.org/10.3847/1538-4357/ad84f7)
- Pacucci, F., Nguyen, B., Carniani, S., Maiolino, R., & Fan, X. 2023, *ApJL*, 957, L3, doi: [10.3847/2041-8213/ad0158](https://doi.org/10.3847/2041-8213/ad0158)
- Park, K., Ricotti, M., Natarajan, P., Bogdanović, T., & Wise, J. H. 2016, *ApJ*, 818, 184, doi: [10.3847/0004-637X/818/2/184](https://doi.org/10.3847/0004-637X/818/2/184)
- Pérez-González, P. G., Barro, G., Rieke, G. H., et al. 2024, *ApJ*, 968, 4, doi: [10.3847/1538-4357/ad38bb](https://doi.org/10.3847/1538-4357/ad38bb)
- Pizzati, E., Hennawi, J. F., Schaye, J., et al. 2025, *MNRAS*, 539, 2910, doi: [10.1093/mnras/staf660](https://doi.org/10.1093/mnras/staf660)
- Polletta, M. d. C., Wilkes, B. J., Siana, B., et al. 2006, *ApJ*, 642, 673, doi: [10.1086/500821](https://doi.org/10.1086/500821)
- Pouliasis, E., Ruiz, A., Georgantopoulos, I., et al. 2024, *A&A*, 685, A97, doi: [10.1051/0004-6361/202348479](https://doi.org/10.1051/0004-6361/202348479)



- Quadri, G., Trinca, A., Lupi, A., Colpi, M., & Volonteri, M. 2025, arXiv e-prints, arXiv:2505.05556, doi: [10.48550/arXiv.2505.05556](https://doi.org/10.48550/arXiv.2505.05556)
- Quataert, E., & Gruzinov, A. 2000, *ApJ*, 539, 809, doi: [10.1086/309267](https://doi.org/10.1086/309267)
- Regan, J. A., Downes, T. P., Volonteri, M., et al. 2019, *MNRAS*, 486, 3892, doi: [10.1093/mnras/stz1045](https://doi.org/10.1093/mnras/stz1045)
- Ricci, C., Trakhtenbrot, B., Koss, M. J., et al. 2017, *Nature*, 549, 488, doi: [10.1038/nature23906](https://doi.org/10.1038/nature23906)
- Richards, G. T., Strauss, M. A., Fan, X., et al. 2006, *AJ*, 131, 2766, doi: [10.1086/503559](https://doi.org/10.1086/503559)
- Riffel, R., Rodríguez-Ardila, A., & Pastoriza, M. G. 2006, *A&A*, 457, 61, doi: [10.1051/0004-6361:20065291](https://doi.org/10.1051/0004-6361:20065291)
- Rinaldi, P., Bonaventura, N., Rieke, G. H., et al. 2025, *ApJ*, 992, 71, doi: [10.3847/1538-4357/adfa10](https://doi.org/10.3847/1538-4357/adfa10)
- Rodríguez-Ardila, A., Viegas, S. M., Pastoriza, M. G., & Prato, L. 2002, *ApJ*, 565, 140, doi: [10.1086/324598](https://doi.org/10.1086/324598)
- Rusakov, V., Watson, D., Nikopoulos, G. P., et al. 2025, arXiv e-prints, arXiv:2503.16595, doi: [10.48550/arXiv.2503.16595](https://doi.org/10.48550/arXiv.2503.16595)
- Sacchi, A., & Bogdán, Á. 2025, *ApJL*, 989, L30, doi: [10.3847/2041-8213/adf5c8](https://doi.org/10.3847/2041-8213/adf5c8)
- Saikia, P., Körding, E., & Falcke, H. 2015, *MNRAS*, 450, 2317, doi: [10.1093/mnras/stv731](https://doi.org/10.1093/mnras/stv731)
- Salpeter, E. E. 1964, *ApJ*, 140, 796, doi: [10.1086/147973](https://doi.org/10.1086/147973)
- Sassano, F., Capelo, P. R., Mayer, L., Schneider, R., & Valiante, R. 2023, *MNRAS*, 519, 1837, doi: [10.1093/mnras/stac3608](https://doi.org/10.1093/mnras/stac3608)
- Satō, H. 1966, *Progress of Theoretical Physics*, 35, 241, doi: [10.1143/PTP.35.241](https://doi.org/10.1143/PTP.35.241)
- Schaerer, D. 2002, *A&A*, 382, 28, doi: [10.1051/0004-6361:20011619](https://doi.org/10.1051/0004-6361:20011619)
- Schaerer, D., Contini, T., & Pindao, M. 1999, *A&AS*, 136, 35, doi: [10.1051/aas:1999197](https://doi.org/10.1051/aas:1999197)
- Schindler, J.-T., Hennawi, J. F., Davies, F. B., et al. 2025, *Nature Astronomy*, doi: [10.1038/s41550-025-02660-1](https://doi.org/10.1038/s41550-025-02660-1)
- Schneider, R., & Maiolino, R. 2024, *A&A Rv*, 32, 2, doi: [10.1007/s00159-024-00151-2](https://doi.org/10.1007/s00159-024-00151-2)
- Scholtz, J., Maiolino, R., D'Eugenio, F., et al. 2025, *A&A*, 697, A175, doi: [10.1051/0004-6361/202348804](https://doi.org/10.1051/0004-6361/202348804)
- Schulze, A., Misawa, T., Zuo, W., & Wu, X.-B. 2018, *ApJ*, 853, 167, doi: [10.3847/1538-4357/aaa7f0](https://doi.org/10.3847/1538-4357/aaa7f0)
- Setton, D. J., Greene, J. E., de Graaff, A., et al. 2024, arXiv e-prints, arXiv:2411.03424, doi: [10.48550/arXiv.2411.03424](https://doi.org/10.48550/arXiv.2411.03424)
- Setton, D. J., Greene, J. E., Spilker, J. S., et al. 2025, *ApJL*, 991, L10, doi: [10.3847/2041-8213/ade78b](https://doi.org/10.3847/2041-8213/ade78b)
- Shakura, N. I., & Sunyaev, R. A. 1973, *A&A*, 24, 337
- Shen, Y., & Ho, L. C. 2014, *Nature*, 513, 210, doi: [10.1038/nature13712](https://doi.org/10.1038/nature13712)
- Sheth, R. K., & Tormen, G. 2002, *MNRAS*, 329, 61, doi: [10.1046/j.1365-8711.2002.04950.x](https://doi.org/10.1046/j.1365-8711.2002.04950.x)
- Shi, X.-H., Jiang, P., Wang, H.-Y., et al. 2016, *ApJ*, 829, 96, doi: [10.3847/0004-637X/829/2/96](https://doi.org/10.3847/0004-637X/829/2/96)
- Shi, Y., Kremer, K., Grudić, M. Y., Gerling-Dunsmore, H. J., & Hopkins, P. F. 2023, *MNRAS*, 518, 3606, doi: [10.1093/mnras/stac3245](https://doi.org/10.1093/mnras/stac3245)
- Shi, Y., Kremer, K., & Hopkins, P. F. 2024, *ApJL*, 969, L31, doi: [10.3847/2041-8213/ad5a95](https://doi.org/10.3847/2041-8213/ad5a95)
- Silverman, J., Li, J., Ding, X., et al. 2025, arXiv e-prints, arXiv:2507.23066, doi: [10.48550/arXiv.2507.23066](https://doi.org/10.48550/arXiv.2507.23066)
- Sołtan, A. 1982, *MNRAS*, 200, 115
- Stone, J. M., Pringle, J. E., & Begelman, M. C. 1999, *MNRAS*, 310, 1002, doi: [10.1046/j.1365-8711.1999.03024.x](https://doi.org/10.1046/j.1365-8711.1999.03024.x)
- Stone, M. A., Lyu, J., Rieke, G. H., Alberts, S., & Hainline, K. N. 2024, *ApJ*, 964, 90, doi: [10.3847/1538-4357/ad2a57](https://doi.org/10.3847/1538-4357/ad2a57)
- Sugimura, K., Hosokawa, T., Yajima, H., & Omukai, K. 2017, *MNRAS*, 469, 62, doi: [10.1093/mnras/stx769](https://doi.org/10.1093/mnras/stx769)
- Takeo, E., Inayoshi, K., & Mineshige, S. 2020, *MNRAS*, 497, 302, doi: [10.1093/mnras/staa1906](https://doi.org/10.1093/mnras/staa1906)
- Tanaka, T. S., Silverman, J. D., Shimasaku, K., et al. 2024, arXiv e-prints, arXiv:2412.14246, doi: [10.48550/arXiv.2412.14246](https://doi.org/10.48550/arXiv.2412.14246)
- Tanaka, T. S., Akins, H. B., Harikane, Y., et al. 2025, arXiv e-prints, arXiv:2508.00057, doi: [10.48550/arXiv.2508.00057](https://doi.org/10.48550/arXiv.2508.00057)
- Tang, M., Stark, D. P., Plat, A., et al. 2025, *ApJ*, 991, 217, doi: [10.3847/1538-4357/adfd57](https://doi.org/10.3847/1538-4357/adfd57)
- Taylor, A. J., Finkelstein, S. L., Kocevski, D. D., et al. 2025a, *ApJ*, 986, 165, doi: [10.3847/1538-4357/add15b](https://doi.org/10.3847/1538-4357/add15b)
- Taylor, A. J., Kokorev, V., Kocevski, D. D., et al. 2025b, *ApJL*, 989, L7, doi: [10.3847/2041-8213/ade789](https://doi.org/10.3847/2041-8213/ade789)
- Tee, W. L., Fan, X., Wang, F., & Yang, J. 2025, *ApJL*, 983, L26, doi: [10.3847/2041-8213/adc5e3](https://doi.org/10.3847/2041-8213/adc5e3)
- Temple, M. J., Hewett, P. C., & Banerji, M. 2021, *MNRAS*, 508, 737, doi: [10.1093/mnras/stab2586](https://doi.org/10.1093/mnras/stab2586)
- Torralba, A., Matthee, J., Pezzulli, G., et al. 2025a, arXiv e-prints, arXiv:2505.09542, doi: [10.48550/arXiv.2505.09542](https://doi.org/10.48550/arXiv.2505.09542)
- . 2025b, arXiv e-prints, arXiv:2510.00103, doi: [10.48550/arXiv.2510.00103](https://doi.org/10.48550/arXiv.2510.00103)
- Tortosa, A., Ricci, C., Ho, L. C., et al. 2023, *MNRAS*, 519, 6267, doi: [10.1093/mnras/stac3590](https://doi.org/10.1093/mnras/stac3590)
- Toyouchi, D., Inayoshi, K., Hosokawa, T., & Kuiper, R. 2021, *ApJ*, 907, 74, doi: [10.3847/1538-4357/abcfce2](https://doi.org/10.3847/1538-4357/abcfce2)
- Trefoloni, B., Ji, X., Maiolino, R., et al. 2025, *A&A*, 700, A203, doi: [10.1051/0004-6361/202452795](https://doi.org/10.1051/0004-6361/202452795)



- Tripodi, R., Bradač, M., D'Eugenio, F., et al. 2025, arXiv e-prints, arXiv:2507.20684, doi: [10.48550/arXiv.2507.20684](https://doi.org/10.48550/arXiv.2507.20684)
- Übler, H., Maiolino, R., Curtis-Lake, E., et al. 2023, A&A, 677, A145, doi: [10.1051/0004-6361/202346137](https://doi.org/10.1051/0004-6361/202346137)
- Ueda, Y., Akiyama, M., Hasinger, G., Miyaji, T., & Watson, M. G. 2014, ApJ, 786, 104, doi: [10.1088/0004-637X/786/2/104](https://doi.org/10.1088/0004-637X/786/2/104)
- Ulrich, M.-H., Maraschi, L., & Urry, C. M. 1997, ARA&A, 35, 445, doi: [10.1146/annurev.astro.35.1.445](https://doi.org/10.1146/annurev.astro.35.1.445)
- Valentini, M., Gallerani, S., & Ferrara, A. 2021, MNRAS, 507, 1, doi: [10.1093/mnras/stab1992](https://doi.org/10.1093/mnras/stab1992)
- Vanden Berk, D. E., Richards, G. T., Bauer, A., et al. 2001, AJ, 122, 549, doi: [10.1086/321167](https://doi.org/10.1086/321167)
- Volonteri, M., & Begelman, M. C. 2010, MNRAS, 409, 1022, doi: [10.1111/j.1365-2966.2010.17359.x](https://doi.org/10.1111/j.1365-2966.2010.17359.x)
- Volonteri, M., Habouzit, M., & Colpi, M. 2021, Nature Reviews Physics, 3, 732, doi: [10.1038/s42254-021-00364-9](https://doi.org/10.1038/s42254-021-00364-9)
- Wang, A., An, T., Zhang, Y., et al. 2023, MNRAS, 525, 6064, doi: [10.1093/mnras/stad2651](https://doi.org/10.1093/mnras/stad2651)
- Wang, B., Leja, J., de Graaff, A., et al. 2024, ApJL, 969, L13, doi: [10.3847/2041-8213/ad55f7](https://doi.org/10.3847/2041-8213/ad55f7)
- Wang, B., de Graaff, A., Davies, R. L., et al. 2025a, ApJ, 984, 121, doi: [10.3847/1538-4357/adc1ca](https://doi.org/10.3847/1538-4357/adc1ca)
- Wang, B., Leja, J., Katz, H., et al. 2025b, arXiv e-prints, arXiv:2508.18358, doi: [10.48550/arXiv.2508.18358](https://doi.org/10.48550/arXiv.2508.18358)
- Wang, J.-M., Watarai, K.-Y., & Mineshige, S. 2004, ApJL, 607, L107, doi: [10.1086/421906](https://doi.org/10.1086/421906)
- Wellons, S., Faucher-Giguère, C.-A., Hopkins, P. F., et al. 2023, MNRAS, 520, 5394, doi: [10.1093/mnras/stad511](https://doi.org/10.1093/mnras/stad511)
- Williams, C. C., Alberts, S., Ji, Z., et al. 2024, ApJ, 968, 34, doi: [10.3847/1538-4357/ad3f17](https://doi.org/10.3847/1538-4357/ad3f17)
- Woods, T. E., Patrick, S., Elford, J. S., Whalen, D. J., & Heger, A. 2021, ApJ, 915, 110, doi: [10.3847/1538-4357/abfaf9](https://doi.org/10.3847/1538-4357/abfaf9)
- Wu, J., Brandt, W. N., Anderson, S. F., et al. 2012, ApJ, 747, 10, doi: [10.1088/0004-637X/747/1/10](https://doi.org/10.1088/0004-637X/747/1/10)
- Xiao, M., Oesch, P. A., Bing, L., et al. 2025, A&A, 700, A231, doi: [10.1051/0004-6361/202554361](https://doi.org/10.1051/0004-6361/202554361)
- Yokoyama, J. 1998, PhRvD, 58, 083510, doi: [10.1103/PhysRevD.58.083510](https://doi.org/10.1103/PhysRevD.58.083510)
- Yu, Q., & Tremaine, S. 2002, MNRAS, 335, 965, doi: [10.1046/j.1365-8711.2002.05532.x](https://doi.org/10.1046/j.1365-8711.2002.05532.x)
- Yuan, F., & Narayan, R. 2014, ARA&A, 52, 529, doi: [10.1146/annurev-astro-082812-141003](https://doi.org/10.1146/annurev-astro-082812-141003)
- Yue, M., Eilers, A.-C., Ananna, T. T., et al. 2024a, ApJL, 974, L26, doi: [10.3847/2041-8213/ad7eba](https://doi.org/10.3847/2041-8213/ad7eba)
- Yue, M., Eilers, A.-C., Simcoe, R. A., et al. 2024b, ApJ, 966, 176, doi: [10.3847/1538-4357/ad3914](https://doi.org/10.3847/1538-4357/ad3914)
- Zackrisson, E., Rydberg, C.-E., Schaerer, D., Östlin, G., & Tuli, M. 2011, ApJ, 740, 13, doi: [10.1088/0004-637X/740/1/13](https://doi.org/10.1088/0004-637X/740/1/13)
- Zakamska, N. L., Schmidt, G. D., Smith, P. S., et al. 2005, AJ, 129, 1212, doi: [10.1086/427543](https://doi.org/10.1086/427543)
- Zhang, Y., Ding, X., Yang, L., et al. 2025a, arXiv e-prints, arXiv:2510.25830, doi: [10.48550/arXiv.2510.25830](https://doi.org/10.48550/arXiv.2510.25830)
- Zhang, Z., Jiang, L., Liu, W., & Ho, L. C. 2025b, ApJ, 985, 119, doi: [10.3847/1538-4357/adc3e](https://doi.org/10.3847/1538-4357/adc3e)
- Zhang, Z., Jiang, L., Liu, W., Ho, L. C., & Inayoshi, K. 2025c, arXiv e-prints, arXiv:2506.04350, doi: [10.48550/arXiv.2506.04350](https://doi.org/10.48550/arXiv.2506.04350)
- Zhu, Q., Li, Y., Li, Y., et al. 2022, MNRAS, 514, 5583, doi: [10.1093/mnras/stac1556](https://doi.org/10.1093/mnras/stac1556)
- Zhuang, M.-Y., & Ho, L. C. 2023, Nature Astronomy, 7, 1376, doi: [10.1038/s41550-023-02051-4](https://doi.org/10.1038/s41550-023-02051-4)
- Zhuang, M.-Y., Li, J., Shen, Y., et al. 2025, arXiv e-prints, arXiv:2505.20393, doi: [10.48550/arXiv.2505.20393](https://doi.org/10.48550/arXiv.2505.20393)